Traffic & Transportation

Coordinated Optimisation Model of Ramp Merging Sequences and Trajectories in Mixed Traffic

Weijing ZHU[1], Sining YU[2], Tao WANG[3], Chaoqiang TIAN[4], Xiongcai GAN[5], Xiaoqin ZHOU[6]

Original Scientific Paper
Submitted: 28 Apr 2025
Accepted: 25 Sept 2025
Published: 27 May 2026

[1] Wlzx@kjt.gxzf.gov.cn, Guangxi Science and Technology Information Network Centre, Nanning, China
[2] 23152202009@mails.guet.edu.cn, School of Architecture and Transportation Engineering, Guilin University of Electronic Technology, Guilin, China
[3] wangtao@guet.edu.cn, Guangxi Key Laboratory of Intelligent Transportation System, Nanning Research Institute, Guilin University of Electronic Technology, Nanning, China
[4] 1256564634@qq.com, School of Architecture and Transportation Engineering, Guilin University of Electronic Technology, Guilin, China
[5] 2062876024@qq.com, School of Architecture and Transportation Engineering, Guilin University of Electronic Technology, Guilin, China
[6] Corresponding author, 42092598@qq.com, Guangxi Transport Vocational and Technical College, Nanning, China

Publisher:
Faculty of Transport and Traffic Sciences, University of Zagreb

ABSTRACT
The long-term coexistence of connected and automated vehicles (CAVs) and human-driven vehicles (HDVs) in mixed traffic flows will continue to significantly impact merging behaviours and operational efficiency in freeway on-ramp merging areas. To improve merging efficiency at freeway on-ramps, this paper proposes a cooperative merging model for mixed traffic. First, the merging points for ramp vehicles are determined based on vehicle interaction characteristics in the merging area. Then, for the dynamic decision-making problem of merging sequences, considering the differences in cooperative merging between CAVs and HDVs, the optimal merging sequence for both single-vehicle and multi-vehicle platoon merging is determined by minimising the global deviation between the actual travel time and the expected minimum travel time. Finally, according to the predetermined merging sequence, a bidirectional speed guidance strategy based on virtual vehicle mapping is designed for both mainline and ramp vehicles to achieve cooperative optimisation of the merging sequence and vehicle trajectories, enabling the smooth merging of ramp vehicles into the mainline. Simulations verify that the proposed method performs better than FIFO and effectively improves merging efficiency under different CAV penetration rates. Particularly in low-to-medium penetration scenarios, it achieves a 25% delay optimisation rate and 22% reduction in travel time, with the optimisation effect improving to varying degrees as penetration rates increase. This establishes a foundation for traffic analysis and cooperative control in freeway on-ramp merging areas under mixed traffic environments.

KEYWORDS
connected and automated vehicles; ramp merging area; vehicle cooperative control methods; mixed traffic.

1. INTRODUCTION

As a critical component of road network topology, the freeway merging area is a typical bottleneck where traffic conflicts frequently arise, leading to decreased traffic efficiency. The high heterogeneity of human driving behaviours and localised information perception impose significant safety and efficiency risks during conventional merging processes, manifested in two primary aspects: (1) potential conflicts between ramp and mainline vehicles persistently occur in freeway on-ramp merging areas, and (2) uncontrolled vehicle inflows cause congestion when downstream road sections exceed capacity. In connected and automated environments,

vehicles can exchange real-time information via vehicle-to-vehicle (V2V) and vehicle-to-infrastructure (V2I) technologies, enabling collaborative coordination between ramp and mainline vehicles. This capability holds promise for alleviating congestion, reducing energy consumption and emissions, and enhancing merging efficiency and safety in freeway on-ramp merging areas. However, due to technological limitations and infrastructure constraints, mixed traffic flows comprising both connected and automated vehicles (CAVs) and human-driven vehicles (HDVs) will persist long-term in connected and automated environments. Consequently, investigating cooperative merging strategies for freeway on-ramp areas under mixed traffic conditions carries substantial theoretical and practical significance.

Freeway merging control directly governs the overall efficiency of traffic flows [1], with existing research categorised into optimal and suboptimal strategies. Yang et al. [2] proposed an integrated platoon control method that pre-allocates vehicle platoons and optimises mainline vehicle speeds via information-sharing technologies, significantly reducing total travel costs while maintaining traffic throughput. Gao et al. [3] developed a platoon splitting cooperative merging (PSCM) method for CAVs, innovatively introducing a platoon splitting mechanism coupled with motion control and effect evaluation modules to address high-demand scenarios on mainlines. Chen et al. [4] advanced beyond conventional single-vehicle matching by formulating a mixed integer nonlinear programming (MINLP) model to determine the optimal number and selection strategy of mainline "facilitator vehicles", systematically mitigating ramp interference. At the implementation level, Karbalaieali et al. [5] proposed a dynamic adaptive algorithm based on travel time cost functions for real-time merging control adjustments, with simulations under varying traffic demands offering novel insights into dynamic scenario adaptability. However, optimal strategies suffer from computational limitations, with solving efficiency plummeting for scenarios involving over 20 vehicles, whereas suboptimal strategies (e.g. average inventory method (AIM) [6], first-in, first-out (FIFO) [7]) generate local optima rapidly but fail to guarantee global efficiency. Xu et al. [8] introduced a group-based strategy to alleviate congestion via vehicle clustering, providing a compromise for multi-vehicle merging sequence coordination.

In fully connected environments where all vehicles are controllable, mixed traffic flows introduce escalating complexity to merging decision-making due to the heterogeneity of human drivers and heterogeneous interactions between CAVs and HDVs. The uncertainty of HDV driving behaviour makes it difficult for traditional merging strategies to accurately predict conflict risks, exacerbating safety and efficiency challenges in merging areas. Game theory has been widely adopted to model such dynamic conflicts. Arbis et al. [9] and Xie et al. [10] constructed an interactive model based on game theory, which transforms the merging problem into a nonlinear optimisation task and achieves safety gap control through real-time acceleration adjustment. Liao et al. [11] validated their game-theoretic strategy via a Unity-SUMO co-simulation platform, demonstrating a 110% increase in traffic flow speed and a 77% reduction in fuel consumption. To address the complexity of mixed traffic flows, hierarchical control frameworks enhance system scalability by decoupling decision-making layers. Han et al. [12] proposed a two-level hierarchical architecture, where the upper layer optimises the CAV trajectory and the lower layer models the HDV behaviour using the Gipps model, achieving collaborative merging of multiple lanes. Bian et al. [13] designed a dual-layer structure to decouple vehicle dynamics control from information interaction, effectively addressing heterogeneous vehicle characteristics. At the operational level, Chen et al. [14] optimised the acceleration of CAVs by combining MPC with third-order vehicle dynamics, while Karimi et al. [15] enhanced merging safety and comfort through cooperative trajectory algorithms. Wang et al. [16] implemented a two-stage cooperative merging strategy in a mixed environment, optimising the cooperative distance at the vehicle level and determining the leading vehicle based on proximity principles to coordinate mainline and ramp traffic. Liu et al. [17] introduced an eco-friendly merging strategy for heterogeneous traffic, synchronising lane decisions and longitudinal speeds via conditional proximal policy optimisation algorithms to balance travel time, energy consumption and emissions. While these frameworks improve modularity, most studies remain confined to full CAV or high-penetration scenarios, with insufficient exploration of CAV-guided HDV mechanisms under low penetration rates.

To address the challenges posed by the uncertainty of HDV behaviour, existing research focuses on utilising the active control capability of CAVs to achieve precise convergence through trajectory optimisation and collaborative decision-making. Cao et al. [18] adopted a model predictive control (MPC) framework to dynamically optimise the merging trajectory by adjusting the speed of mainline vehicles and the acceleration of ramp vehicles, significantly improving the control accuracy of the merging point. Mu et al. [19] further proposed an event-triggered rolling horizon trajectory planning method, partitioning the merging area into pre-merging, virtual merging and execution sub-regions. By leveraging mixed-integer nonlinear programming (MINLP) to generate optimal trajectories, their experiments demonstrated the robustness of this approach in mixed traffic

flows, with trajectory correction capabilities strengthening as CAV penetration rates increase. Xu et al. [20] focused on hybrid electric vehicles, designing torque distribution strategies to reduce energy consumption, thereby providing novel insights for eco-friendly traffic control. Notably, Yang et al. [21] derived the optimal longitudinal control analytical solution for multi-lane scenarios based on cooperative game theory, synchronously optimising driving efficiency and fuel economy. Wu et al. [22] further developed a longitudinal dynamics-based trajectory optimisation model, employing the Pontryagin minimum principle (PMP) algorithm to determine optimal control inputs, achieving smooth ramp vehicle merging. However, existing studies predominantly assume fixed gaps in mainline traffic or stable traffic states, exhibiting limited adaptability to dynamic traffic density fluctuations and neglecting cascading disturbance effects caused by single-vehicle merging on subsequent traffic.

In summary, current research on merging area collaborative control remains constrained by three interrelated limitations: the decoupled optimisation of merging sequences and trajectories, insufficient adaptability to CAV penetration rates and unquantified spatiotemporal conflict propagation. Traditional approaches, such as rule-based strategies [23] and dynamic programming methods [24], prioritise computational simplicity or fixed trajectory assumptions but fail to dynamically synchronise sequence decisions with real-time traffic state variations, particularly under fluctuating CAV adoption levels. To address these challenges, this paper proposes a joint optimisation method for the freeway on-ramp merging sequence and trajectory. First, by analysing the behaviour of vehicles entering the freeway on-ramp merging area, the merging point is identified. Then, considering the differences between CAVs and HDVs, cooperative merging rules are established. Aiming to minimise the deviation between vehicles' actual passing time and the expected shortest time, this method determines the optimal merging order for both single vehicles and platoons, ensuring safe ramp merging. Finally, integrating two-way speed regulation for mainline and ramp vehicles, a speed guidance method based on virtual vehicle mapping is developed. Through numerical simulations compared with the classic FIFO method, the proposed control strategy is verified to enhance passage efficiency, effectively cut delays and stops, and boost vehicle safety. The main contributions of this paper can be categorised as follows: (1) the proposed method introduces a dynamic merging sequence optimisation strategy for dual merging points, ensuring a high merging success rate through the verification of the length of the speed adjustment area and the scheduling of extreme scenarios, and (2) a layered architecture for spatiotemporally coupled order decision-making and vehicle cooperative control is developed to achieve simultaneous optimisation of merging priority assignment and trajectory parameters, including acceleration and safety spacing.

The rest of this paper is organised as follows. Section 2 describes the proposed optimisation model for the motorway ramp merging area. Section 3 describes the process of simulation verification of the ramp merging area vehicle cooperative optimisation model by designing experiments. Finally, Section 4 offers some concluding remarks.

2. SYSTEM FRAMEWORK AND METHODOLOGY

This section outlines the systematic framework and methodological approach proposed in this study to tackle the challenges of highway on-ramp merging in mixed traffic conditions. It explains the hierarchical control strategy, the analysis of merging behaviour based on real-world data, and the coordinated algorithms developed for sequencing and speed guidance, ensuring a comprehensive and effective solution for enhancing merging efficiency and safety.

2.1 Problem formulation

In mixed traffic environments with CAVs and HDVs, traditional merging strategies struggle to accommodate the stochastic behaviours of HDVs and fluctuating traffic densities. Freeway ramp merging areas face critical challenges, including insufficient single-vehicle cooperation efficiency, pronounced multi-vehicle conflict and uncoordinated control, leading to traffic congestion and energy waste. To enhance merging efficiency and energy conservation, this paper proposes a proactive cooperative control and speed guidance methodology. By analysing vehicle merging behavioural characteristics, designing single-vehicle collaboration rules and multi-vehicle platoon coordination strategies, and developing cooperative speed guidance protocols for mainline and ramp vehicles, the proposed method addresses traffic bottleneck issues in complex merging scenarios.

The study focuses on cooperative merging behaviours within a single ramp merging area. Based on merging characteristics, the merging area is subdivided into three sub-areas: pre-merging area, speed adjustment area and merging area, as illustrated in *Figure 1*.

1) Pre-merging area: Upon entering this area, a centralised controller generates merging sequences based on real-time traffic states.
2) Speed adjustment area: CAVs adjust speeds to align with target gaps via direct control commands, while HDVs respond indirectly to guidance signals.
3) Merging area: Lane-changing trajectory planning ensures merging safety.

The length of the pre-merging area should be determined by the road's speed limit and the maximum comfortable deceleration, as calculated by the following formula:

$$l_{\text{pre}} = \frac{V_{\max}^2}{|2 \cdot a_{\text{co}}|} \tag{1}$$

where l_{pre} represents the length of the pre-merging area (m), $V_{\max}$ is the maximum speed limit of the road (m/s) and a_{co} is the comfortable acceleration/deceleration rate of the vehicle (commonly taken as ±2.2 m/s²).

In the speed adjustment area, to ensure the merging sequence proceeds safely, let us assume the scheduling time in the speed adjustment area is T . When vehicles from the mainline and the ramp arrive at the trigger point of the speed adjustment area simultaneously, in order to guarantee that vehicles can maintain an appropriate safety gap when exiting this area for merging, it is necessary to set a safety lower limit for the scheduling time T. The specific calculation formula is as follows:

$$\left(\frac{1}{2}a_{\text{m}}T^2 - V_{\text{m}}T\right) - \left(V_{\text{r}}T + \frac{1}{2}b_m T^2\right) \geq L_{ch} + d_{\text{sfd}} \tag{2}$$

where a_{m} and b_m are the maximum deceleration and acceleration (m/s²), respectively; V_{m} and V_{r} represent the maximum speeds of the mainline and ramp vehicles (m/s), respectively; L_{ch} and d_{sfd} are the length of the vehicle platoon (m) and the minimum safe distance (m). The assumption of constant velocities V_{m} , V_{r} during T in *Eq. (2),* provides a conservative lower bound for scheduling time under worst-case scenarios. In actual control execution, dynamic speed adjustments via CAV coordination compensate for this simplification, ensuring real-time safety.

To ensure the safety of merging, a dynamic safety gap is proposed, and the calculation formula is as follows:

$$d_{\text{sfd}} = \varphi v_i(t) + d_{\text{sta}} \tag{3}$$

where d_{sta} represents the distance (m) that vehicle i should maintain with the vehicle in front when stationary; φ is the reaction time (s), and $v_i(t)$ is the speed of vehicle i; in this paper, $v_i(t)$ is set to the maximum mainline speed.

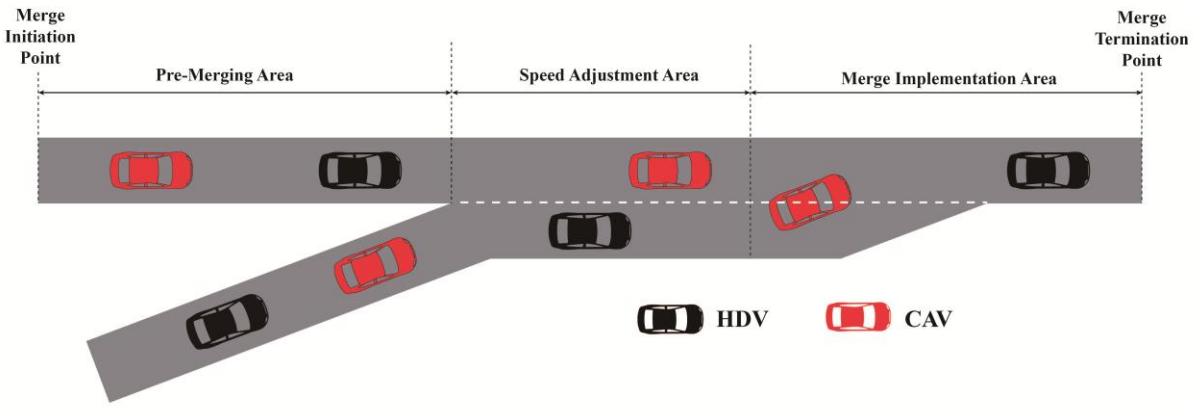

Figure 1 – Merging area considered in the study

Considering that the length of the pre-merging area should be determined by the road's speed limit and maximum comfortable deceleration, and the length of the speed adjustment zone should meet the driving needs of vehicles in the shortest scheduling time, we set the length of the speed adjustment zone to 230 metres, the length of the mainline pre-merging area to 220 metres, and the length of the ramp pre-merging area to 180 metres to ensure safety redundancy.

A cooperative merging control scenario is constructed for the merging of a single-lane mainline and an acceleration lane ramp in freeway environments. The following assumptions are defined:

1) The traffic environment includes a single-lane mainline and an acceleration lane ramp for passenger vehicles only, with no adverse weather conditions or lateral vehicle movements considered.
2) Mixed traffic flow is present, with CAV penetration rates between 1% and 99%, and CAVs receive centralised control commands via vehicle-to-infrastructure (V2I) communication, while HDVs follow car-following models for longitudinal motion.
3) CAV speeds are acquired in real time with high precision, while HDV states are indirectly perceived through roadside units (RSUs) or neighbouring CAVs, with negligible communication latency.
4) Drivers have moderate skill levels, strictly follow traffic rules, and maintain safe inter-vehicle distances during merging manoeuvres.

2.2 Analysis of merging vehicle behaviour

We leveraged the Next Generation Simulation (NGSIM) dataset, sourced from the United States, which includes comprehensive traffic data from two highway segments, namely US-101 and I-80, in addition to two urban roadways. The dataset was captured through a network of seven cameras strategically positioned to cover the study area. Specifically, Camera 1 was tasked with recording the southernmost extremity of the area, focusing on the outermost lane, while Camera 7 was responsible for capturing the northernmost section, which includes the ramp. The data collection spanned a five-hour period from 2:00 PM to 7:00 PM, during which digital video images were meticulously recorded at a frame rate of 10 frames per second. The transcription of vehicle trajectories from these videos provided a detailed dataset encompassing various parameters such as vehicle identification numbers, timestamps, velocities, accelerations, spatial coordinates and lane positions.

For the merging zone analysed (corresponding to segments of US-101 and I-80), the posted speed limit for mainline freeways is 105 km/h. However, under congested conditions (especially in Scenario 3, *Table 1*), actual average speeds (e.g. 25.52 km/h for the outer lane) are significantly lower than this limit. This discrepancy highlights the impact of merging manoeuvres, traffic volume and congestion on real-world speed performance.

For the purposes of this analysis, we extracted highway merge data from three distinct time intervals within the dataset, each corresponding to a unique traffic volume scenario. These scenarios are further elaborated upon in *Table 1*.

Table 1 – Classification of different traffic scenarios

Scenario	Description	Data collection time
Scenario 1	The traffic flow on the mainline and the ramp is relatively stable, with no congestion occurring.	16:00—16:15
Scenario 2	The traffic is in a transition phase from stable to congested, experiencing slight congestion.	17:00—17:15
Scenario 3	Vehicles on both the mainline and the ramp are already congested.	17:15—17:30

As shown in *Figure 2,* the NGSIM vehicle trajectory dataset (1,757 vehicles) was analysed across a 1,750-metre merging zone during congestion. Lane-specific patterns emerge: inner lane trajectories show high consistency with stable speeds (mean variation <2%), indicating minimal merging interference. Middle lane vehicles exhibit trajectory dispersion and 18-22% speed reductions downstream due to exiting ramps and lane changes. Outer lane trajectories demonstrate severe disorder with 35-40% abrupt speed drops in the core merging area, triggering upstream-propagating congestion consistent with traffic shockwave theory.

To further clarify vehicle speed characteristics, we extracted average speeds for mainline lanes from the trajectory data:

1) Inner lane: Exhibits high consistency with stable speeds (mean variation < 2%), averaging 45.49 km/h. This indicates minimal merging interference, as vehicles maintain steady travel without frequent deceleration.
2) Middle lane: Shows trajectory dispersion and 18–22% speed reductions downstream (average speed: 32.54 km/h). The decline is attributed to exiting ramps and moderate merging interactions.

3) Outer lane: Demonstrates severe disorder with 35–40% abrupt speed drops in the core merging area, resulting in an average speed of 25.52 km/h. This lane is most impacted by ramp-to-mainline merging, leading to frequent deceleration and congestion propagation.

The congestion evolution comprises three phases: (1) Initial phase: competitive lane-changing conflicts in the outer lane initiate localised congestion; (2) Escalation phase: speed instability spreads to the middle lane, expanding the congestion footprint; (3) Saturation phase: persistent stop-and-go conditions dominate the outer lane, while intensified exit-ramp lane changes induce middle-lane oscillations, creating coupled "merging-diverging" bottlenecks. This instability stems from three interacting factors: dual traffic loading on the outer lane (mainline + ramp), conservative merging behaviour by human-driven vehicles exacerbating ramp queues, and upstream transmission of congestion waves through vehicle interactions.

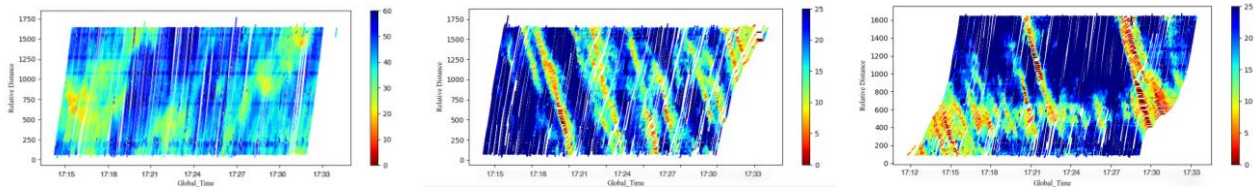

(a) *(b)* *(c)*

Figure 2 – Comparison of spatiotemporal trajectories across lanes: a) Inner lane of the mainline; b) Middle lane of the mainline; c) Outer lane of the mainline

Additionally, as shown in *Figure 3*, based on the lane ID change threshold and peak period vehicle trajectory data statistics, the spatiotemporal distribution patterns of longitudinal merging behaviour in ramp merging areas are revealed. The study shows that within the first 40 metres of the merging area, 85% of vehicles do not initiate lane change behaviour, indicating that ramp vehicles are still in the speed adjustment phase, needing to accelerate and synchronise with the mainline traffic flow to reduce merging risks. The 60-80 m interval accounts for 40% of the merging behaviour, reflecting that vehicles tend to complete the merge quickly after matching speeds to minimise merging time costs. In the end zone (>80 metres), merging behaviour accounts for 10%, primarily due to insufficient gaps in the mainline traffic flow, forcing ramp vehicles to either extend their waiting time or adopt urgent merging strategies. This distribution pattern reveals the dynamic characteristics of the merging gap acceptance threshold: as vehicle speed approaches that of the mainline, drivers' gap acceptance increases significantly. Conversely, when there is a greater speed discrepancy, merging decisions are delayed due to safety risk aversion.

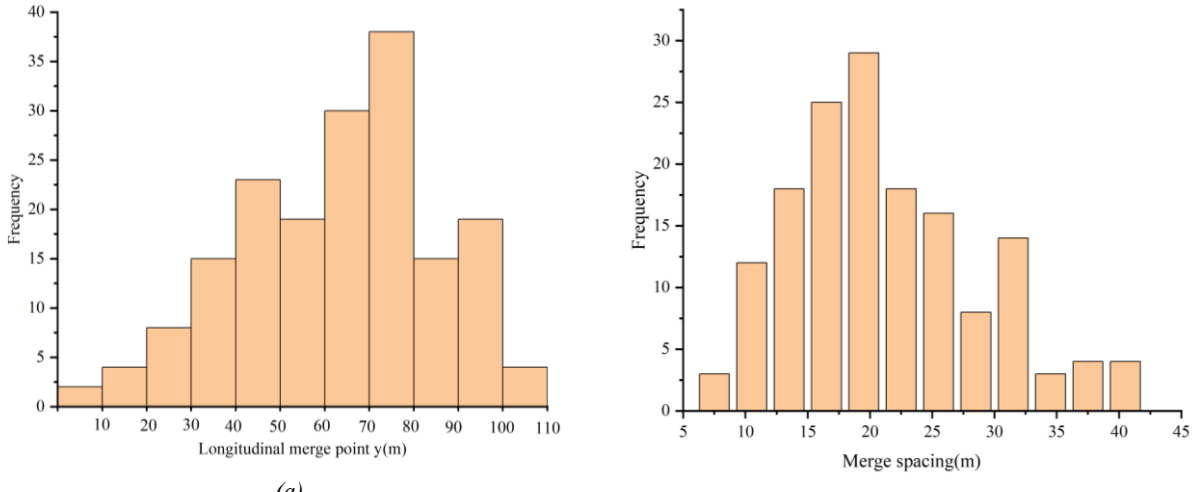

(a) *(b)*

Figure 3 – Spatiotemporal distribution of longitudinal merging behaviour in ramp merging areas: a) Frequency distribution of longitudinal merge point positions for vehicles; b) Frequency distribution of lane change gap intervals for vehicles

Leveraging space headway data sourced from the NGSIM dataset, which quantifies the inter-vehicle distance between the centre of the current vehicle and that of the preceding vehicle, we conduct an in-depth analysis of the gap characteristics in the vicinity of the target lane during the vehicle lane-changing process

(*Figure 4a*). For ramp-entering vehicles, the mean acceptable gap is determined to be 21.57 metres, with a notable 80.67% of these gaps falling below the 25-metre threshold. As the merge point, defined as the spatial locus where the lane-changing manoeuvres are initiated, approaches the terminal segment of the acceleration lane, there is a discernible decline in the gap demand, which underscores a strategic transition in driving behaviour from a conservative waiting mode to a more aggressive merging strategy. Regarding *Figure 4b*, with the x-axis representing the forward gap and the y-axis denoting the backward gap, the observed weak correlation between the forward and backward gaps unveils a unilateral constraint preference inherent in drivers' decision-making processes – specifically, for a lane change to be triggered, it suffices for only one of the two gaps (either the front or the rear gap) to satisfy the pre-established threshold condition, rather than requiring the simultaneous optimisation of both gap parameters.

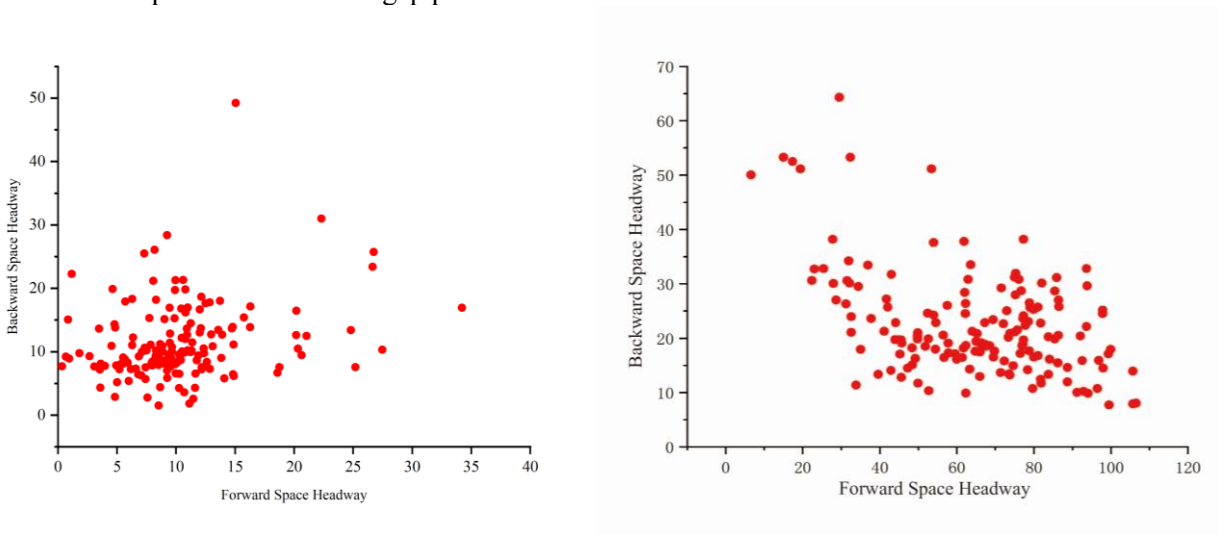

(a) *(b)*

Figure 4 – Correlation between forward and backward gaps during lane changes: a) Scatter plot of merge points and merge gaps; b) Scatter plot of forward versus backward gaps for lane-changing vehicles.

2.3 Decision-making of ramp merging sequences

To address the complexity of collaborative control in merging areas under mixed traffic flow environments, a hierarchical merging strategy framework is constructed. The system prioritises CAVs as lead vehicles during queue formation, dynamically splitting queues when exceeding five vehicles or exhibiting mismatched headways. HDVs maintain fixed following without active adjustment. Merging sequences are optimised via rolling 2-second updates – this period is defined based on three key rationales: (1) human driving behaviour constraints, aligning with the average reaction time of HDVs (1.5–2.5 seconds); (2) CAV control stability, covering V2X communication latency (0.3–0.8 seconds) plus vehicle dynamic response time (0.5–1.2 seconds); and (3) traffic flow fluctuation characteristics, where 2 seconds serves as the critical threshold for quasi-steady-state traffic conditions. Upon entering the pre-merge zone, vehicles' merge-point arrival times are predicted using kinematic models. This informs multi-criteria sequencing that integrates mainline priority and first-come-first-served principles with real-time traffic states. CAV-involved merges trigger cooperative control, while HDV-only interactions retain natural driving behaviour.

The control module employs dual merge-point fault tolerance, as shown in *Figure 5.* (1) Primary merge point: defined as an ideal position in the speed adjustment area under normal traffic gaps. This location is determined by comprehensively considering traffic flow characteristics, vehicle manoeuvrability, and safety verification through traffic simulation. Traffic-flow characteristics are based on quasi-steady-state threshold analyses. Vehicle manoeuvrability involves matching HDV reaction time and CAV dynamic response requirements. At this point, vehicles (both CAVs and HDVs) have sufficient conditions for speed adaptation and traffic state perception to conduct safe merging. (2) Secondary merge point: activated when insufficient gaps at the primary merge point necessitate CAV behavioural compensation. This adaptive mechanism aligns with real-world traffic dynamics, where vehicles may adjust merging positions due to changing traffic gaps. CAVs mitigate HDV uncertainty through adaptive gap management, decelerating to accommodate conservative HDVs or accelerating to counter aggressive ones, ensuring merge feasibility.

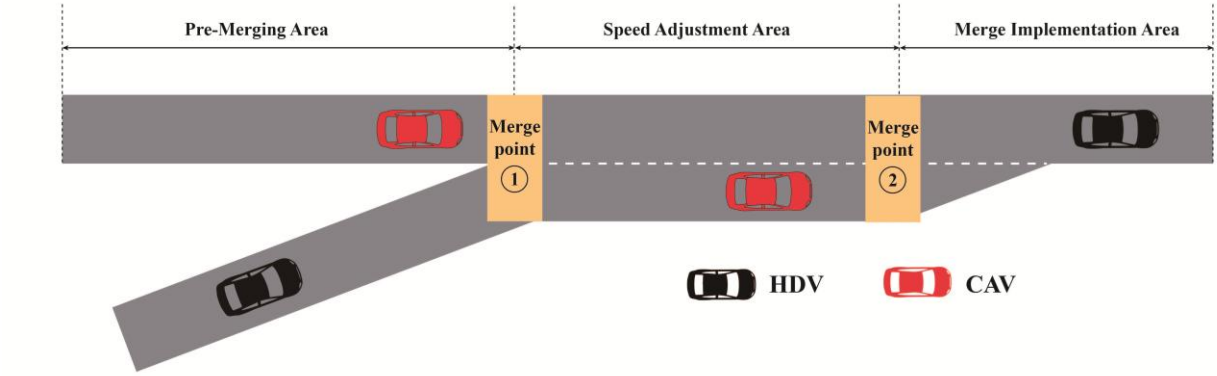

Figure 5 – Distribution of vehicle collaborative merging points.

The cooperative merging strategy for mixed traffic flows addresses two key scenarios: CAV-CAV and CAV-HDV interactions. For CAV-CAV merging, a dynamic priority negotiation mechanism governs operations at the primary merge point. In Stage 1, CAVs exchange real-time kinematic data (position, speed, acceleration) via V2V communication to assess spatiotemporal urgency. If the ramp CAV exhibits higher urgency, the system triggers "ramp priority" mode, prompting the mainline CAV to decelerate and widen safety gaps; conversely, "mainline priority" mode delays merging via ramp CAV trajectory adjustments. Stage 2 employs nonlinear programming to calculate optimal safe time windows once priorities are assigned, ensuring collision-free synchronisation at the merge point through coordinated speed and gap management. This two-phase protocol maintains adaptive decision-making while preserving natural traffic flow principles.

After determining the priority, the system ensures that both vehicles meet safety conditions when they reach merge point ① as follows:

$$\begin{cases} min(v_{t_{e,i}}^{i} - v_{t_{e,i}}^{i\text{-}1}) \\ x_{t_{e,i}}^{i} - x_{t_{e,i}}^{i\text{-}1} \geq v_{t_{e,i}}^{i\text{-}1} \cdot T_{min,1} \end{cases} \tag{4}$$

where $v_{t_{e,i}}^{i}$ and $x_{t_{e,i}}^{i}$ are the speed and the position of vehicle i at time $t_{e,i}$, and $T_{\min,1}$ is the minimum headway distance for CAV vehicles during merging. e denotes the merge-point-related critical time index. The parameter $t_{e,i}$ denotes the exact time instant at which vehicle i reaches the primary merge point (merge point ①), serving as a critical temporal anchor for evaluating safety constraints during the merging manoeuvre.

If t_e^{i-1}-$t_e^i \leq T_{\min,1}$, meaning that the time gap between vehicles passing the merge point is smaller than the required minimum time, a speed adjustment strategy is triggered. The formula for this calculation is:

$$a_{i-1} = \frac{(T_{\min,1} \cdot v_{t_{e,i}}^{i-1} + x_{t_{e,i}}^{i-1} - x_{t_{e,i}}^{i}) - v_{t_{e,i}}^{i-1}(t_e^i - t)}{0.5 \cdot (t_e^i - t)^2} \tag{5}$$

where a_{i-1} is the acceleration of the vehicle, t represents the current calculation moment, which is the real-time timestamp when the system generates control instructions and serves as the starting time reference for kinematic calculation. $t_e^i - t$ stands for the remaining time, which is the time interval from the current moment to the planned merging time, and it is used to calculate the decision-making time window required for deceleration.

To ensure the efficiency of mainline traffic, a minimum speed limit of 40 km/h is set in this study. If the following vehicle, using the mainliner's maximum deceleration rate, cannot meet merging conditions at the merge point or reach the speed limit, it should merge at merge point ② instead. When the following vehicle decelerates to the merge point, it can meet the merging conditions of the preceding vehicle. Upon entering the speed adjustment area, speed control is applied, similar to merge point ①, where the following vehicle reduces its speed. Speed and acceleration are calculated using the motion equation provided in the following formula:

$$v_{i-1} = \sqrt{2a'_{e,i-1}\left(T_{\min,1} \cdot v_{i-1}^{t-1} + x_{i-1}^{t-1} - x_{i-1}^{t}\right) - \left(v_{i-1}^{t-1}\right)^2} \tag{6}$$

$$a'_{i-1}=a_{co} \tag{7}$$

The negative sign in the kinetic energy term $-(v_{i-1}^{t-1})^2$ reflects the energy dissipation during braking. Here, $a'_{e,i-1}$ is defined as a positive scalar representing the magnitude of deceleration. Where v_{i-1}, a'_{i-1} and a_{co} are the speed of the following vehicle when it reaches merge point ②, the deceleration of the following vehicle and the comfortable deceleration rate for CAV vehicles, respectively.

For the CAV-HDV mixed traffic flow merging scenario, the collaborative merging methods can be divided into the following two situations: (1) the mainline CAV yields to the ramp HDV, and (2) the ramp CAV yields to the mainline HDV. The roadside unit (RSU) continuously monitors the vehicle states in the merging area (position, speed, acceleration) and transmits the HDV trajectory prediction data to the CAVs via V2I communication. The CAV, combining its own sensors with the RSU information, adjusts its acceleration or deceleration actions to maintain an appropriate safety gap. The "mainline CAV yielding to ramp HDV" scenario is used here as an example for further explanation.

Assuming the previous vehicle is an HDV, denoted as H_i, and the roadside unit (RSU) is equipped with monitoring or sensing devices, the time it takes for the vehicle to reach the merge point can be estimated as:

$$t_{hdv}^{i} = t_0 + \frac{L - x_{t_0}^{i}}{v_{t_0}^{i}} \tag{8}$$

where t_0 is the detection start time, defined as the initial moment when the roadside unit (RSU) first detects vehicle i in the merging area. t_{hdv}^{i} and L are the estimated time for the vehicle to reach the merge point ① and the length of the merging area. Additionally, $x_{t_0}^{i}$ and $v_{t_0}^{i}$ are the position and speed of vehicle i at time t_0.

At time t_{hdv}^{i}, the speed and position of the following vehicle $i-1$ can be obtained through vehicle-to-vehicle (V2V) communication. To ensure safety and improve efficiency, the time gap between the preceding and following vehicles at the merge point must be greater than the minimum required time for safe merging, as expressed by the following formula:

$$\begin{cases} min(v_{t_{hdv,i}}^{i} - v_{t_{hdv,i}}^{i-1}) \\ t_{cav}^{i-1} - t_{hdv}^{i} \geq T_{\min,2} \end{cases} \tag{9}$$

where t_{cav}^{i-1}, $T_{\min,2}$ and $v_{t_{hdv,i}}^{i}$ are the time for the following CAV to reach the merge point ①, the minimum headway distance between CAV and HDV vehicles during merging and the speed of the preceding vehicle at time t_{hdv}^{i}.

If the time gap for merging is smaller than the minimum required for safe merging, the vehicle should enter a speed control mode to adjust its speed, taking into account the lack of active control capabilities in HDV vehicles. The following vehicle reduces its speed according to the following equation:

$$a_{i-1} = \frac{(T_{\min,2} \cdot v_{t_{hdv,i}}^{i-1} + x_{t_{hdv,i}}^{i-1} - x_{t_{hdv,i}}^{i}) - v_{t_{hdv,i}}^{i-1}(t_{hdv}^{i} - t_0)}{0.5 \cdot (t_{hdv}^{i} - t_0)^2} \tag{10}$$

Mirroring CAV-CAV merging logic, vehicles unable to achieve safe merging conditions at the primary merge point under maximum permissible deceleration are redirected to the secondary merge point. The speed adjustment zone ensures sufficient safety gaps between mainline and ramp vehicles through mandatory deceleration upon entry. This protocol aligns merging speeds with preceding vehicles via kinematic calculations, maintaining operational consistency with primary merge point controls while prioritising gap stability over positional optimisation. The system enforces trajectory synchronisation through physics-based speed modulation rather than spatial prioritisation, ensuring compatibility across merge scenarios. According to the principles of kinematics, speed and acceleration can be calculated using the corresponding formula.

$$v_{i-1} = \sqrt{2a'_{i-1}(T_{\min,2} \cdot v_{t_{hdv,i}}^{i-1} + x_{t_{hdv,i}}^{i-1} - x_{t_{hdv,i}}^{i}) - (v_{t_{hdv,i}}^{i-1})^2} \tag{11}$$

$$a'_{i-1} = a_{co} \tag{12}$$

where v_{i-1}, a'_{i-1} and a_{co} are the speed of the following vehicle when it reaches merge point ②, the deceleration of the following vehicle and the comfortable acceleration/deceleration rate for the vehicle.

To fully leverage the active control role of CAV, the study proposes a CAV-led multi-vehicle platoon cooperative control method, comprising two core modules: (1) platoon formation and (2) passage sequence

optimisation, to achieve efficient and safe merging processes. A queueing strategy with a CAV is proposed as the lead vehicle to regulate HDV behaviour using its communication and stability. The maximum queue length is limited to 5 vehicles, and the CAV penetration threshold is set at 20% to prevent regulation failure or excessive safety spacing at low penetration rates. The desired headway spacing under stable following conditions is given by:

$$h_d^{ij} = 6.588 \cdot e^{0.1021 V^{i-1,j}} \tag{13}$$

The constants 6.588 and 0.1021 are empirically derived from Yang Longhai et al.'s study [25] on steady-state car-following behaviour. These values were calibrated through statistical analysis of traffic datasets, characterising the relationship between platoon lead-vehicle speed $V^{i-1,j}$ and safe headway:

6.588: Baseline headway (meters) at reference speed, embedding minimum safety margins.

0.1021: Sensitivity coefficient quantifying the exponential growth of desired headway with speed.

For CAV vehicle N_i and the preceding vehicle N_{i-1}, the headway distance h_i is determined as follows: h_d^i represents the desired headway for CAV vehicle N_i. It is the expected safe distance that should be maintained from the preceding vehicle under stable following conditions, calculated by *Formula 13,* considering factors like vehicle speed.

(1) If $h_i \le h_d^i$, the CAV vehicle can maintain a safe following distance and join the preceding CAV queue. (2) If $h_i > h_d^i$, the CAV vehicle does not meet the vehicle following condition and will merge into a new CAV queue as the last vehicle.

The queue construction protocol prioritises CAVs as lead vehicles, with roadside units dynamically adjusting platoon configurations. When a CAV follows, the desired headway is calculated using real-time positioning and target spacing. Queues exceeding five vehicles trigger new CAV-led platoon formation, while excessive desired headways prompt merging with preceding queues to optimise safety and throughput.

Order optimisation is a core issue in ramp merging studies. In this study, the objective is to minimise the total time vehicles spend in the speed adjustment area, and an optimal decision model is developed based on multiple constraints. The model defines the expected arrival time of vehicles on the ramp and mainline (shortest independent passage time) under an interference-free scenario, and minimises the global deviation between the actual allocated time and the expected time to achieve dynamic optimisation of the merging sequence. At the same time, constraints such as maximum speed limits, safe following distance thresholds, and mandatory lane change distances are introduced to ensure that the model balances the physical feasibility of traffic flow and the safety of driving behaviour.

1) The shortest time for ramp vehicles to reach the merging area

When a ramp vehicle enters the pre-merge area, it actively forms a platoon. It is assumed that the traffic flow entering the ramp is free-flowing, and the starting time for the passage order decision is the time at which the vehicle first enters the pre-merge area. After the lead CAV vehicle on the ramp completes the platooning, its speed adjustment mode is divided into two types: (1) acceleration stage. The lead CAV first accelerates toward the maximum speed limit, utilising the maximum allowable acceleration. During this stage, speed increases continuously until reaching v_{max}. (2) Constant speed stage. Once the maximum speed limit is achieved, the lead CAV transitions to maintaining a constant speed, where acceleration drops to 0 (no further speed change). The calculation formula for the lead vehicle is as follows:

$$v_{fm}^{ramp} = \min\left(v_{\lim}^{ramp}, v_0 + t_0 a_{\max}\right) \tag{14}$$

where v_{fm}^{ramp}, $v_{\lim}^{ramp}$, v_0, t_0 and $a_{\max}$ are the speed of the ramp vehicle when the platoon completes, the maximum speed limit of the ramp, the initial speed of the CAV lead vehicle when it enters the merge area, the platoon formation time and the maximum acceleration of the lead vehicle.

When the CAV lead vehicle completes platooning, the travelling distance based on the speed follows two conditions, calculated as:

$$L_{de}^{ramp} = \begin{cases} v_0 t_0 + \dfrac{1}{2} a_m t_0^2 & v_{fm} < v_{\lim}^{ramp} \\ v_{\lim}^{ramp}\left(t_0 - \dfrac{v_{\lim}^{ramp} - v_0}{a_m}\right) + \dfrac{\left(v_{\lim}^{ramp}\right)^2 - v_o^2}{2a_m} & v_{fm} = v_{\lim}^{ramp} \end{cases} \tag{15}$$

where a_m represents the maximum acceleration rate for the ramp vehicle, L_{de}^{ramp} is the distance travelled by the platoon when the lead vehicle completes platooning.

When the platoon completes, the vehicle adjusts to maximum acceleration until it reaches the maximum ramp speed, then the following vehicle completes its merge accordingly. The shortest time for the platoon to pass the merge area can be calculated by:

$$T_{ad}^{ramp} = \frac{v_{\lim}^{main} - v_{\lim}^{ramp}}{b_m} + \frac{L_{ad}^{ramp} - \left(\frac{\left(v_{\lim}^{main}\right)^2 - \left(v_{\lim}^{ramp}\right)^2}{2b_m}\right)}{v_{\lim}^{main}} \tag{16}$$

where b_m represents the maximum acceleration rate for the mainline vehicle, T_{ad}^{ramp} and $v_{\lim}^{main}$ are the shortest time for the platoon to pass through the merge area and the maximum speed limit of the mainline.

The entire set of formulas leads to the calculation of the minimum time for the CAV lead vehicle to enter the merging area and reach the speed adjustment area. The calculation formula is as follows:

$$T_{\min}^{ramp} = T_{pre}^{ramp} + T_{ad}^{ramp} \tag{17}$$

where $T_{\min}^{ramp}$ is the shortest time for the platoon of vehicles to enter the merging area.

2) The shortest time for mainline vehicles to reach the merging area

When the CAV lead vehicle and the mainline vehicle are aligned, and the CAV is recognised as part of the platoon, the speed change can be achieved in two scenarios. The lead vehicle accelerates to the maximum mainline speed, and the lead vehicle makes speed adjustments. When the platoon completes, the lead vehicle's speed is calculated as follows:

$$v_{fm}^{main} = \min\left(v_{\lim}^{main}, v_0 + t_0 b_{\mathrm{m}}\right) \tag{18}$$

where v_{fm}^{main} and $v_{\lim}^{main}$ are the speed of the lead vehicle when the platoon completes and the maximum speed limit of the mainline.

Based on the CAV lead vehicle completing the platoon, the distance travelled and the speed are calculated as follows:

$$L_{de}^{\mathrm{main}} = \begin{cases} v_0 \mathrm{t}_0 + \frac{1}{2} b_m t_0^2 & v_{fm}^{main} < v_{\lim}^{ramp} \\ v_{\lim}^{main}\left(t_0 - \frac{v_{\lim}^{main} - v_0}{b_m}\right) + \frac{\left(v_{\lim}^{main}\right)^2 - v_o^2}{2b_m} & v_{fm}^{main} = v_{\lim}^{ramp} \end{cases} \tag{19}$$

where L_{de}^{main} is the distance travelled by the lead vehicle in the platoon when the lead vehicle completes.

Considering the maximum speed in the platoon area and the maximum acceleration until reaching the maximum mainline speed, the following calculation is made:

$$T_{\min}^{main} = \begin{cases} \mathrm{t}_0 + \frac{v_{\lim}^{main} - v_{fm}^{main}}{b_m} + \frac{L_{pre}^{main} + L_{ad}^{main} - L_{de}^{main} - \left(\frac{\left(v_{\lim}^{main}\right)^2 - \left(v_{fm}^{main}\right)^2}{2b_m}\right)}{v_{\lim}^{main}} & v_{fm}^{main} < v_{\lim}^{main} \\ \mathrm{t}_0 + \frac{L_{pre}^{main} + L_{ad}^{main} - L_{de}^{main}}{v_{\lim}^{main}} & v_{fm}^{main} = v_{\lim}^{main} \end{cases} \tag{20}$$

where $T_{\min}^{main}$ is the shortest time for the lead vehicle to enter the merging area.

3) Passage order optimisation model

To achieve the dual goals of enhancing both efficiency and safety in merging areas, this paper constructs an optimisation model structured to synergise hard safety constraints and efficiency-oriented objectives. Safety is first guaranteed through non-negotiable constraints (e.g. minimum time gaps and dynamic safety distances) that strictly prevent unsafe states, defining a "safe solution space" where all feasible trajectories avoid collision risks. Within this pre-validated safe domain, the model targets efficiency by minimising the total time vehicles spend in the speed adjustment area, operationally, which translates to reducing the global deviation between vehicles' actual and expected passing times. Key parameters, including each vehicle's arrival time at the merging zone and the desired merging distance, guide the optimisation to balance local manoeuvrability and network-wide traffic flow. By embedding safety as rigid bounds and efficiency as the core objective, the model ensures that performance improvements never compromise fundamental safety requirements. The optimisation formula, reflecting this integrated design, is presented as follows:

$$\min \sum_{i=1}^{K} t_{acc}^{i} - t_{\min}^{i}, i = 1,2.\ldots K \tag{21}$$

where K , t_{acc}^{i} and $t_{\min}^{i}$ are the total number of vehicle platoons, the passing time of the vehicle platoon and the shortest required passing time for the vehicle platoon.

Vehicles must adhere to lane speed limits and their own physical motion constraints. To prevent unrealistic vehicle allocation times, upper and lower bounds for assigned times must be established. This involves calculating the shortest and longest times for a vehicle to reach the merging point. The longest time is calculated by assuming the vehicle passes through the area at maximum speed before switching to the minimum speed limit to reach the merging point. The specific constraint formulas are as follows:

$$t_{\min}^{i} \le t_{acc}^{i} \le t_{\max}^{i}, i = 1,2.\ldots K \tag{22}$$

where $t_{\min}^{i}$ and $t_{\max}^{i}$ are the shortest time based on maximum acceleration and the longest time calculated based on the minimum speed limit.

When two vehicles merge, to ensure safety, the distance between them must meet the minimum safety gap required for merging. There are generally two cases when two vehicles pass through the merging point, including cases in which both vehicles are in the same lane and cases in which vehicles merge from different lanes and the vehicles merge from different lanes. When vehicles from the same lane pass through the merging point, the time headway must satisfy the following equation:

$$|t_k^a - t_l^a| \ge \Delta t_2 + \Delta t_3, k \in [1,2\ldots n_1], l \in [1,2\ldots n_2] \tag{23}$$

where Δt_2 denotes the minimum inter-lane merging time gap (set to 2.0 s), which is larger than the intra-lane merging time gap Δt_1 due to increased complexity in cross-lane interactions. Δt_3 represents the time for a platoon's trailing vehicle to pass the merging point, calculated as:

$$\Delta t_3 = \frac{L_{ch\mathrm{i}}}{v_{re}} \tag{24}$$

where $L_{ch\mathrm{i}}$ is the platoon length, and v_{re} is the trailing vehicle's speed, derived from the ACC car-following model:

$$a_{ij}(t) = k_a\left[h_{ij}(t) - l_{ij} - d_0 - V_{ij}(t) \cdot h_d^{ij}\right] + k_b \cdot \left|V_{ij}(t) - V_{i-1,j}(t)\right| \tag{25}$$

where k_a, k_b are the control system coefficients, $a_{ij}(t)$ is the acceleration of vehicle i in platoon j at time t , d_0 and h_d^{ij} are the minimum spacing threshold and desired headway.

The platoon length $L_{ch\mathrm{i}}$ is determined by the number of vehicles. For a single-vehicle platoon, $L_{ch\mathrm{i}}$ equals the vehicle length. For multi-vehicle platoons, it is defined as the positional difference between the leader and trailing vehicle.

$$L_{ch\mathrm{i}} = \begin{cases} L_{ch} & i = 1 \\ L_n - L_{n-1} & i > 1 \end{cases} \tag{26}$$

2.4 Model formulation

To address discontinuous constraints in merging sequence optimisation for mixed traffic flows, this study proposes a Big-M method-based mixed-integer programming (MIP) model. Building on the continuous decision variable t_{acc}^{i} (acceleration time), a binary variable a_{kl} is introduced to represent the precedence relationship between adjacent lane vehicles k (mainline) and l (ramp) at the merging point. The formulated model is as follows:

$$\min \sum_{i=1}^{K} t_{acc}^{i} - t_{\min}^{i}, i = 1,2.\ldots K \tag{27}$$

$$t_{acc}^{i} \le t_{\max}^{i}, i = 1,2.\ldots K \tag{28}$$

$$t_{acc}^{i} \geq t_{\min}^{i}, i = 1,2.\ldots K \tag{29}$$

$$t_{i}^{a} - t_{i-1}^{a} \geq \Delta t_1, i \in 1,2.\ldots K \tag{30}$$

$$t_{k}^{a} - t_{l}^{a} + M \times a_{kl} \geq \Delta t_2 + \Delta t_3, k \in [1,2\ldots n_1], l \in [1,2\ldots n_2] \tag{31}$$

$$t_{l}^{a} - t_{k}^{a} + M \times (1 - a_{kl}) \geq \Delta t_2 + \Delta t_3, k \in [1,2\ldots n_1], l \in [1,2\ldots n_2] \tag{32}$$

$$a_{kl} = \begin{cases} 0, t_k^a \geq t_l^a \\ 1, t_k^a < t_l^a \end{cases} \tag{33}$$

The model is solved using a branch-and-bound algorithm, where M denotes a sufficiently large integer. For $a_{kl} = 0$, constraint (32) becomes active, enforcing lane-changing compliance when the mainline vehicle k merges later than the ramp vehicle l. Conversely, $a_{kl} = 1$ prioritises the mainline vehicle. While the computational complexity scales with the number of vehicles in the pre-merging area, the framework strategically reduces this burden through a platoon-based optimisation strategy. By computing only the arrival time of platoon leaders and enforcing fixed intra-platoon spacing constraints, the problem scale is effectively reduced from vehicle-level to platoon-level, enabling independent sequencing of platoons while maintaining area-wide coordination. This approach transforms the complexity landscape, ensuring real-time feasibility for a typical merging area with up to 5 platoons by leveraging road geometry constraints to limit problem size. Warm-start initialisation and variable reduction techniques further enhance computational efficiency, streamlining the optimisation process without introducing additional symbols.

2.5 Vehicle speed guidance methods in the merge area

To achieve safe and efficient merging of vehicles according to a preset passage order, this section proposes a collaborative control framework based on virtual vehicle mapping. This framework is combined with a bidirectional speed control strategy for mainline and ramp vehicles (*Figure 6)*. The merging point is set as the origin, and the ramp platoon is virtually projected onto the adjacent lane of the mainline, forming a unified control space. Real-time vehicle position, speed and distance to the merging point are obtained through DSRC/LTE-V communication between the RSU and the CAVs. The mainline and ramp platoons are integrated into a virtual queue, with each vehicle assigned a unique number based on the preset passage order, ensuring the merging process is organised.

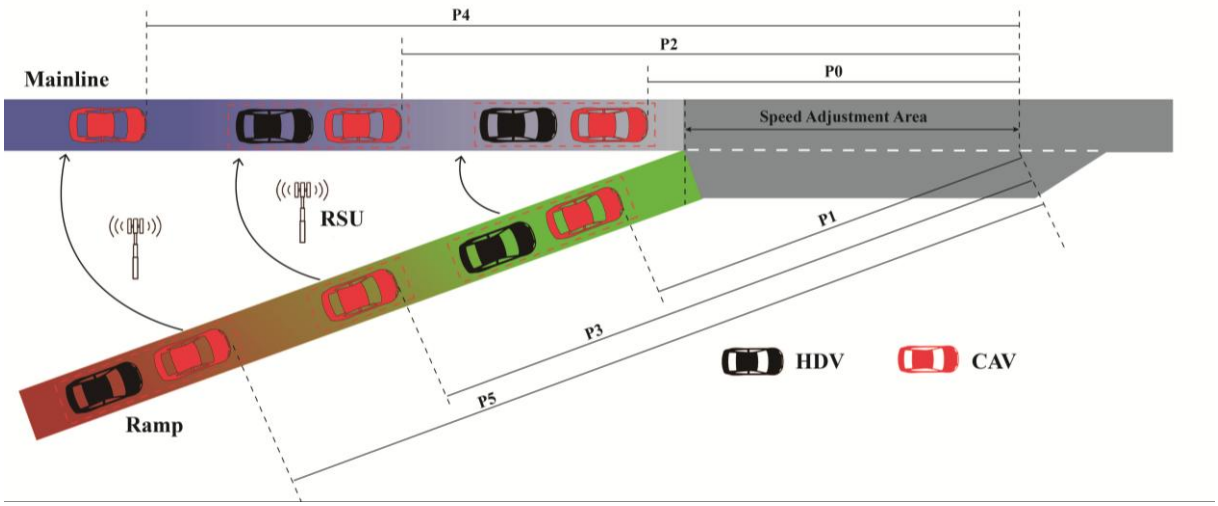

Figure 6 – Diagram of virtual vehicle mapping principle

For the three merging failure scenarios of ramp vehicles: insufficient rear gap, insufficient front gap and insufficient bidirectional gap, four types of collaborative control strategies are designed (*Table 2*): maintaining constant speed, deceleration of mainline following vehicles, acceleration of mainline leading vehicles, and acceleration of both the mainline leading and following vehicles. *Figure 7* shows the spatio-temporal trajectory diagram of the mainline vehicle speed decision.

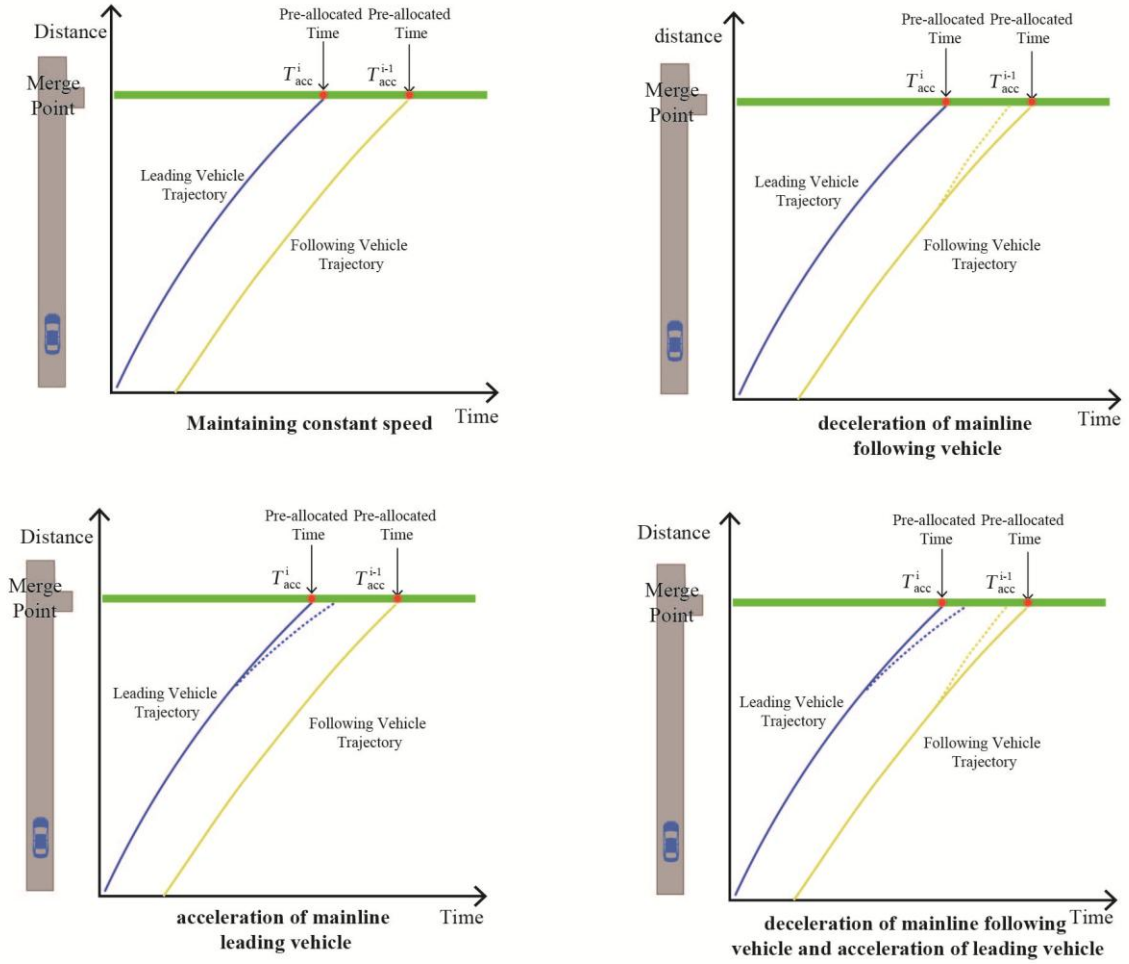

Figure 7 – Speed decision trajectories of mainline vehicles under cooperative merging controls

Table 2 – Mainline vehicle collaborative speed decision

Judgment condition mathematical expression	**Collaborative control strategy**	**Target speed (m/s) / Acceleration (m/s²)**
$d_{mer} \geq S_{accept}$ $d_{leader} \geq S_{leader}$ $d_{follow} \geq S_{follow}$	Mainline vehicle maintains its current motion state	Mainline vehicle speed and acceleration remain unchanged
$d_{mer} \geq S_{accept}$ $d_{leader} < S_{leader}$ $d_{follow} \geq S_{follow}$	Leading vehicle accelerates, following vehicle maintains speed	$v'_{follow} = \sqrt{v^2_{follow} - 2a'_i(S_{follow} - d_{follow})}$ $a'_i = a_{co}$
$d_{mer} \geq S_{accept}$ $d_{leader} \geq S_{leader}$ $d_{follow} < S_{follow}$	Leading vehicle maintains speed, following vehicle decelerates	$v'_{leader} = \sqrt{v^2_{leader} - 2a'_j(S_{leader} - d_{leader})}$ $a'_j = a_{co}$
$d_{mer} < S_{accept}$ $d_{leader} < S_{leader}$ $d_{follow} < S_{follow}$	Leading vehicle accelerates, following vehicle decelerates	$v'_{leader} = \sqrt{v^2_{leader} - 2a'_j(S_{accept} - d_{mer} - d_{follow})}$ $a'_j = a_{co}$

Based on the actual arrival time, t^i_{act} and the preset allocated time t^i_{acc}, this section adopts two approaches for adjusting the speed (*Table 3)*: the ramp vehicle head accelerates to the maximum speed, or the ramp vehicle head decelerates to the target speed. *Figure 8* represents the trajectory of the speed adjustment decision.

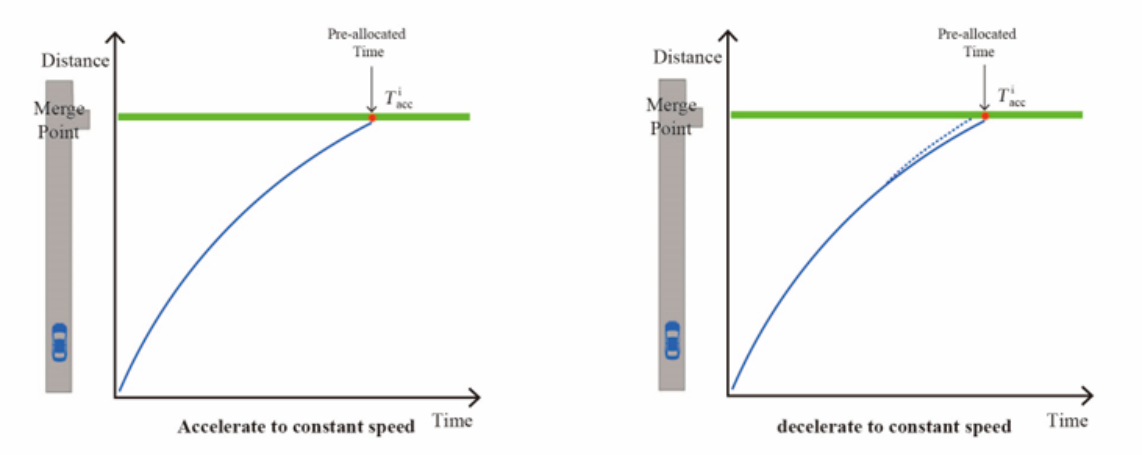

Figure 8 – Speed adjustment decision trajectories for ramp vehicles

Table 3 – Ramp platoon lead vehicle speed decision

Judgment condition mathematical expression	Collaborative control strategy	Target speed (m/s) / Acceleration (m/s²)
$t^i_{act} > t^i_{acc}$	Ramp lead vehicle decelerates to a constant speed	$v'_{ramp} = \sqrt{2a_{ramp}(v_{ramp}\Delta t + 0.5a_{ramp}(\Delta t)^2) + v^2_{ramp}}$ $a_{ramp} < 0$
$t^i_{act} < t^i_{acc}$	Ramp lead vehicle accelerates to a constant speed	$v'_{ramp} = \sqrt{2a_{ramp}(v_{ramp}\Delta t + 0.5a_{ramp}(\Delta t)^2) + v^2_{ramp}}$ $a_{ramp} > 0$

The target speed for ramp vehicles is derived from the kinematic equation $v^2 = u^2 + 2as$, where displacement s during time interval Δt is calculated as: $s = v_{ramp}\Delta t + 0.5a_{ramp}(\Delta t)^2$. This yields: $v'_{ramp} = \sqrt{2a_{ramp}(v_{ramp}\Delta t + 0.5a_{ramp}(\Delta t)^2) + v^2_{ramp}}$ explicitly linking velocity changes to spatial displacement during acceleration/deceleration. Physically, this formulation combines the initial velocity v_{ramp} with acceleration-induced velocity change over Δt, consistent with uniform acceleration kinematics. For collaborative control, mainline vehicle dynamics are characterised by: v_{follow} and v_{leader} represent speeds of mainline following and leading vehicles, with a_i and a_j denoting their accelerations during collaborative control. Spatial parameters d_{mer}(inter-platoon spacing), d_{leader} and d_{follow} (ramp-to-mainline platoon distances), alongside safety thresholds S_{leader}, S_{follow} and S_{accept} (minimum merging clearance). For ramp vehicles, v'_{ramp} and a_{ramp} govern collaborative speed and acceleration adjustments, while Δt quantifies deviations between actual and allocated merging times. These parameters collectively ensure synchronised platoon operations through velocity matching and adaptive gap management.

3. SIMULATION RESULTS AND DISCUSSION

This section presents the simulation experiments and analysis conducted to validate the effectiveness of the proposed cooperative merging strategy. It explains the design of the simulation scenarios, details the results of vehicle trajectory coordination, and evaluates the system performance using key traffic metrics, ensuring a comprehensive assessment of the model's impact on merging efficiency and safety under various conditions.

3.1 Experiment design

The study validates the cooperative merging strategy through 50 simulation trials (10 schemes × 5 repetitions), comparing control groups (human-driven baselines) with experimental groups implementing first-come-first-served, single-vehicle and multi-vehicle collaborative control under 20-80% CAV penetration rates. A 1.5 km I-80 freeway merging zone is modelled using NGSIM data, divided into pre-merge (220 m mainline/180 m ramp) and speed adjustment zones (230 m each). Mainline traffic flows at 1,792 veh/h, while ramp

flow varies hourly from 704 to 1,104 veh/h. Vehicle generation follows time-dependent input flows with intervals dynamically adjusted to match target rates: $\Delta t = \frac{3600}{Q}, Q \in [704,1104]$, where Q is the hourly flow rate. Minimum headways of 1.8 s (CAV) and 2.5 s (HDV) are maintained per FHWA guidelines. Uniform arrivals provide a conservative evaluation baseline, with sensitivity analyses confirming <6% deviation from stochastic arrival models. Initial speeds are set at 80 km/h (mainline) and 60 km/h (ramp), monitored over 4,200 s simulations (600 s warm-up, 3,600 s data collection at 1 s resolution) to ensure trajectory precision.

Driving behaviours are simulated using the Wiedemann99 model for HDVs and the enhanced intelligent driver model (EIDM) for CAVs, with parameters calibrated from established physiological-psychological studies. The experimental framework employs custom seeding to maintain reproducibility while testing spatial-temporal constraints across four CAV adoption levels, ensuring systematic evaluation of merging efficiency under escalating demand scenarios. Key parameters are referenced from the study by Kesting, A [26] and integrated into the merged parameter table (covering VISSIM driving parameters and EIDM-specific parameters), as shown in *Table 4*. The EIDM-specific parameters for CAV control logic are crucial for accurately modelling the behaviour of connected and automated vehicles. These parameters not only govern the acceleration, deceleration and following-distance-keeping of CAVs but also interact with the surrounding traffic environment, as shown in the merged parameter table. The table uniformly presents HDV basic driving parameters, CAV-adapted parameters and corresponding literature links, clearly reflecting the synergy between models and parameter logic.

Table 4 – Parameter table for simulating HDV and CAV driving behaviours

Parameter name		Default value	Range	Actual value
Average expected stop distance		1.50 m	0.50 m~2.50 m	1.85 m
Desired vehicle head distance		0.90 s	0.70 s~2.00 s	1.05 s
Reaction time	CAV	-	-	0.05 s
	HDV	-	0.7 s~2.1 s	1.15 s
Following-vehicle oscillation distance		4.00 m	2.00 m~8.00 m	3.84 m
Enter vehicle status time		-8.00 s	-10.00 s~-2.00 s	-7.60 s
Tight status vehicle oscillation distance		0.35 s	0.05 s~2.00 s	0.55 s
Acceleration rate		0.25 m/s^2	0 m/s^2~2.00 m/s^2	0.85 m/s^2
Desired speed		120 km/h	80 km/h~120 km/h	95 km/h
Congestion distance		2.0 m	1.0 m~3.0 m	1.8 m
Desired deceleration		2.0 m/s^2	1.5 m/s^2~3.0 m/s^2	2.0 m/s^2
Coolness factor		0.99	0.95~1.0	0.98

The experiment used normalised core indicators, with data obtained from VISSIM output files, with data obtained via online real-time collection and analysis using the VISSIM output files: (1) Average vehicle delay: the average traffic delay for the entire traffic flow; (2) Average vehicle speed: the average speed of vehicles during the merging process; (3) The total number of vehicles passing the merge area successfully; (4) The total time it takes for a vehicle to enter the merging area from the current area.

3.2 Simulation results of vehicle trajectory

Based on the NGSIM dataset and simulation trajectory data, this study uses spatio-temporal diagrams (*Figure 9*) to quantitatively analyse the dynamic traffic flow characteristics in the merging area under different control strategies. The scatter sampling interval in the diagrams is 1 second, with a jet colour map used to reflect speed variations, where warm colours represent low speeds and cool colours represent high speeds. The diagrams display the relationship between vehicle speed changes and the spatiotemporal trajectory, with merging points located at 150 m and 370 m, and data from 0-4,200 simulation seconds is used, with the first 600 s allocated as the warm-up period.

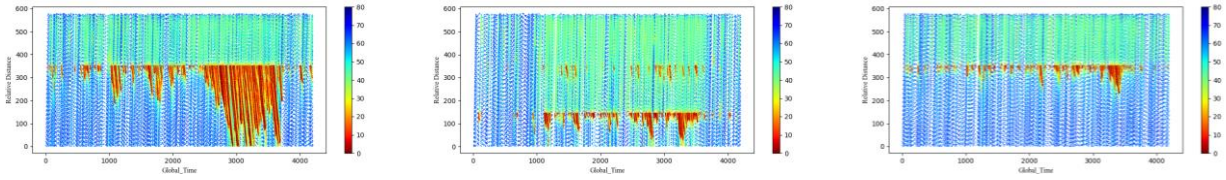

(a) *(b)* *(c)*

Figure 9 – Spatiotemporal diagrams under different control strategies: a) Current trajectory; b) Single-vehicle merging control trajectory; c) Multi-vehicle collaborative control trajectory

From the uncontrolled scenario diagram (*Figure 9a*), it is observed that the three increases in ramp flow (704 → 1,104 veh/h) directly lead to upstream congestion on the mainline. After each increase in flow, the mainline traffic quickly enters a congested state, with vehicle queue lengths increasing by 40%-60% and average speeds dropping to 15-20 km/h. After the congestion alleviates, the mainline traffic remains highly sensitive, and even small disturbances (such as a ramp flow returning to 704 veh/h) can trigger secondary congestion, indicating that natural traffic flows lack stability. At 20% CAV penetration, the proposed single-vehicle merging control marginally alleviates congestion, increasing mainline speed by 12%, yet HDV interactions persist in causing localised bottlenecks. In contrast, the multi-vehicle collaborative method significantly enhances traffic flow efficiency by leveraging CAV-led platoons to synchronise trajectories, reducing conflicts and collision risks. This approach improves road utilisation while lowering energy consumption and emissions. Further spatio-temporal trajectory analyses at 40% and 60% penetration rates (*Figure 10a, 10b*) demonstrate the scalability of both control strategies. The results highlight the multi-vehicle method's superior adaptability in low-penetration scenarios, effectively mitigating queue overflow during peak periods despite HDV dominance.

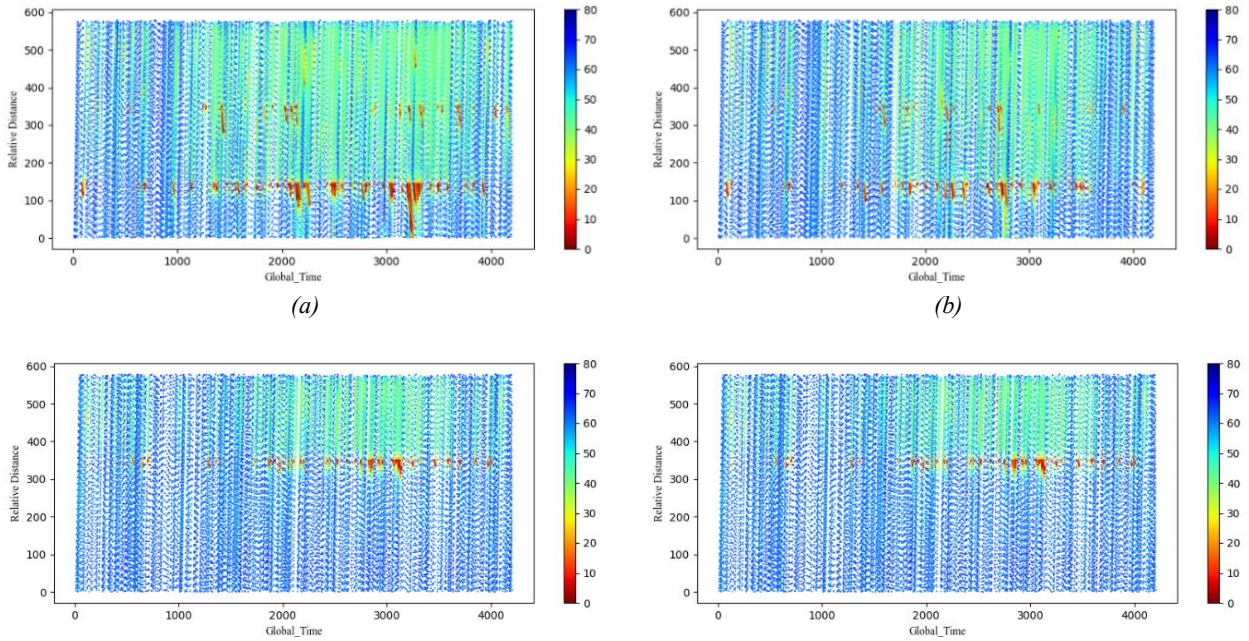

(a) *(b)* *(c)* *(d)*

Figure 10 – Spatiotemporal diagrams of trajectories under different control methods at different penetration rates: a) 40% Single-vehicle; b) 60% Single-vehicle; c) 40% Multi-vehicle; d) 60% Multi-vehicle

From the diagrams, it is clearly observed that as the CAV penetration rate increases to 60%, the single-vehicle merging control shows a significant improvement in optimising mainline traffic, with congestion limited to local road sections (*Figures 10a, 10b)*. he core mechanism behind this is that the increased proportion of CAVs enhances real-time status sharing and collaborative trajectory optimisation between vehicles. V2V communication enables conflict prediction, and CAV-led traffic can dynamically adjust acceleration to smooth speed fluctuations, thereby enhancing traffic flow stability. In comparison, multi-vehicle collaborative control performs optimally in low penetration rate scenarios (20%-40%), with a 48% reduction in congestion length, but its marginal benefits gradually diminish as penetration rates increase (*Figures 10c, 10d)*. This is because sin-

gle-vehicle merging control already resolves over 80% of conflicts at the vehicle level, with remaining optimisation potential focused on extremely dense traffic flow scenarios. Multi-vehicle collaborative control (MCM), on the other hand, needs to handle multi-objective games between vehicle platoons, and as the penetration rate increases, the algorithm's complexity rises while the incremental benefits diminish.

3.3 Simulation evaluation metrics

This section will validate the single-vehicle merging and multi-vehicle collaborative control method for ramp merging areas under scenarios with the same and different penetration rates. The results will be compared with those of the no-control scenario and traditional sequence optimisation methods to verify the effectiveness of the algorithms.

1) Control strategy results analysis under the same penetration rate

Since intelligent connected vehicles are not yet widely deployed on freeways, this study uses a road simulation with a 20% penetration rate of CAVs to align with real-world scenarios. The specific strategies are shown in *Table 5*.

Table 5 – Specific experimental strategies description

Strategy	Description
Strategy 1	Road has fully human-driven vehicles, no control strategy applied.
Strategy 2	Road has mixed traffic flow, no control strategy applied.
Strategy 3	Road with mixed traffic flow, FIFO order optimisation.
Strategy 4	Road with mixed traffic flow, single-vehicle control strategy.
Strategy 5	Road with mixed traffic flow, multi-vehicle collaborative control strategy.

From the evaluation results of each strategy (*Table 6*), it is evident that the introduction of CAVs and their control strategies significantly optimise traffic flow efficiency. Compared to fully human-driven vehicles (Strategy 2), the mixed traffic flow with no control (Strategy 3) shows improvements in average delay, travel time, number of vehicles passing and number of stops, indicating that the collaborative driving characteristics of CAVs have a positive impact on traffic flow. After further applying control strategies, the optimisation effects are more pronounced: the single-vehicle merging control (Strategy 4) reduces average delay by 34.83% compared to the no-control scenario, while the multi-vehicle collaborative control (Strategy 5) further optimises the average delay to 104.60 seconds, a 43.56% improvement over Strategy 2. This indicates that the collaborative control strategy, through real-time interaction between vehicles, effectively reduces merging conflicts and stop-and-go phenomena.

Table 6 – Ramp platoon lead vehicle speed decision

Strategy	Average delay (s)	Average travel time (s)	Vehicles passed	Average number of stops
Strategy 1	185.33	201.17	1518	11.76
Strategy 2	169.16	188.04	1554	10.24
Strategy 3	151.54	180.79	1598	9.66
Strategy 4	104.60	142.21	1717	5.60
Strategy 5	91.16	136.51	1723	4.42

The following comparison charts (*Figure 11*) display the specific values and trends of passage time-related evaluation metrics. The blue bars represent the experimental results for the average delay, average travel time, total number of vehicles passing and average number of stops for each experimental scenario, while the red lines represent the optimisation rates of the metrics.

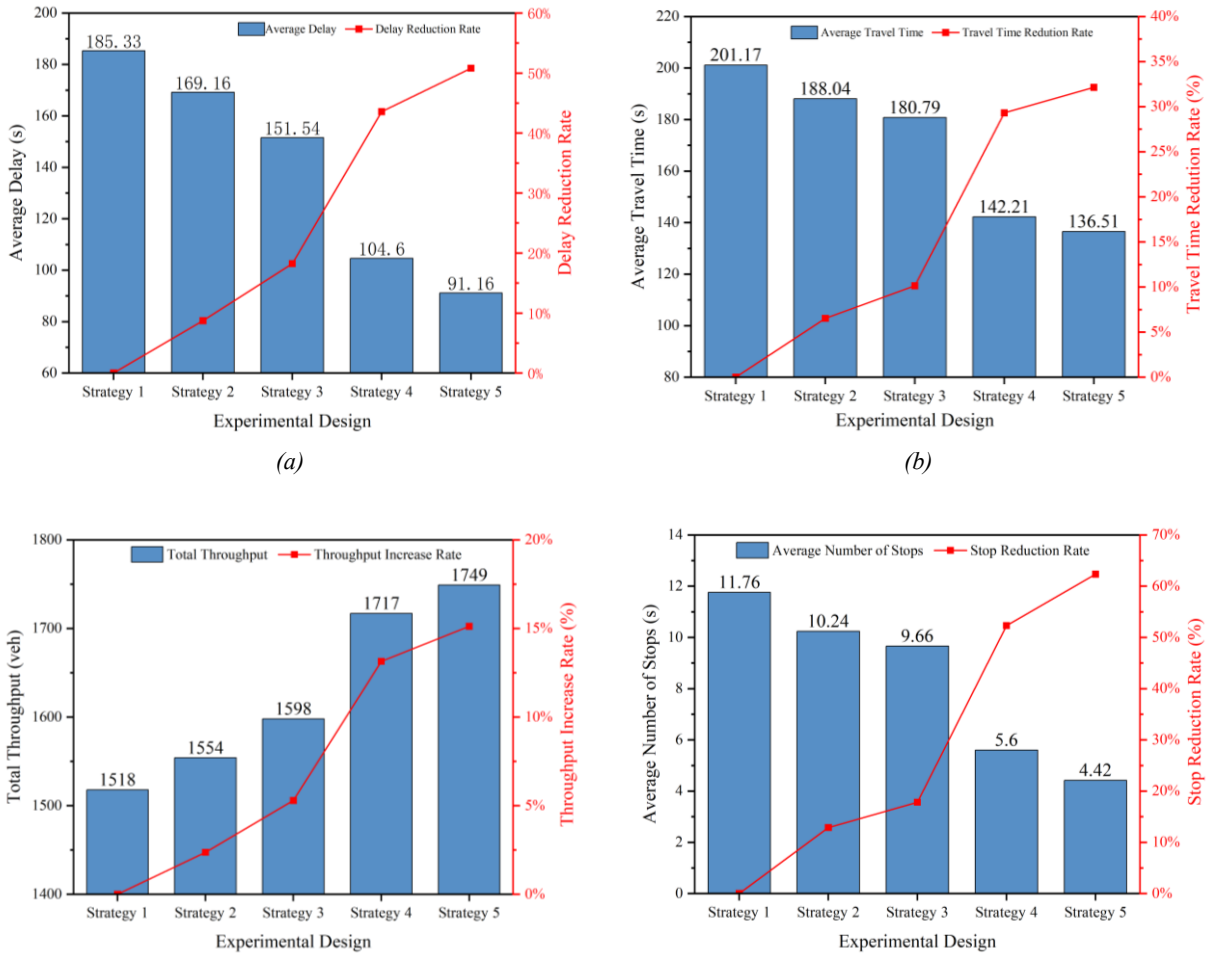

Figure 11 – Comparison of experimental evaluation metrics under different strategies: a) Average delay; b) Average travel time; c) Total throughput; d) Average number of stops

At 20% CAV penetration, control strategies exhibit distinct optimisation effects. Uncontrolled mixed traffic reduces average delay by 8.72% and travel time by 6.53% compared to fully human-driven scenarios, demonstrating CAVs' inherent conflict mitigation capabilities. The first-come-first-served strategy further improves performance, achieving 18.23% delay reduction and 10.13% travel time savings through standardised merging sequences. However, multi-vehicle collaborative control outperforms all methods, reducing delays by 50.81% and travel times by 32.14% versus uncontrolled scenarios. This stems from dynamic speed adjustments and platoon-wide coordination, which minimise stop-and-go waves and stabilise following behaviour.

While total throughput improvements remain modest due to ramp capacity limits, collaborative strategies reduce vehicle stops by 34.47% compared to FIFO by pre-emptively adjusting merging states. The multi-vehicle approach proves optimal in low-penetration scenarios, balancing efficiency gains with congestion suppression through global platoon synchronisation. Its ability to harmonise lead vehicle guidance and follower speed modulation addresses both localised conflicts and mitigates traffic oscillations, establishing a robust framework for mixed traffic optimisation.

2) Control strategy results analysis under different penetration rates

The study evaluates control strategies across CAV penetration rates (20-80%), revealing progressive optimisation gains with higher adoption. For instance, Strategy 5 reduces average delay from 91.96 seconds at 20% penetration to 62.76 seconds at 80%, achieving a 31.7% improvement. However, marginal benefits diminish as CAV prevalence rises. At lower rates, multi-vehicle coordination mitigates traffic instability by harmonising interactions between human-driven and connected vehicles. Beyond 60% penetration, platoons dominated by CAVs exhibit limited incremental gains, narrowing performance differences between advanced and baseline strategies due to inherent system stabilisation from widespread CAV integration.

Table 7 – Ramp platoon speed decision metrics across CAV penetration rates

Experimental	Average delay (s)	Average travel time (s)	Vehicles passed	Average number of stops
Strategy 4 (20%)	107.20	142.21	1717	5.60
Strategy 4 (40%)	87.45	120.83	1834	4.51
Strategy 4 (60%)	77.34	108.79	1880	3.89
Strategy 4 (80%)	69.91	96.19	1958	3.28
Strategy 5 (20%)	91.96	126.03	1749	4.42
Strategy 5 (40%)	76.24	108.97	1896	3.73
Strategy 5 (60%)	68.72	101.90	1989	3.53
Strategy 5 (80%)	62.76	91.68	2020	2.95

The research results show that with the increase in CAV penetration rate, the combined application of passage order optimisation and collaborative control strategies significantly reduces the average vehicle delay, travel time and number of stops, while improving network throughput efficiency. Compared to using only passage order optimisation, the joint strategy yields better overall optimisation results, but the optimisation improvement shows a nonlinear change due to the differences in traffic conditions at different penetration rates.

Figure 12 displays the trends in changes of relevant evaluation metrics and the enhancement of optimisation effects under different CAV penetration rates. The orange bars represent the experimental results of the metrics with passage order optimisation only, the blue bars represent the experimental results with the joint optimisation method, and the red line represents the optimisation rate of the metrics.

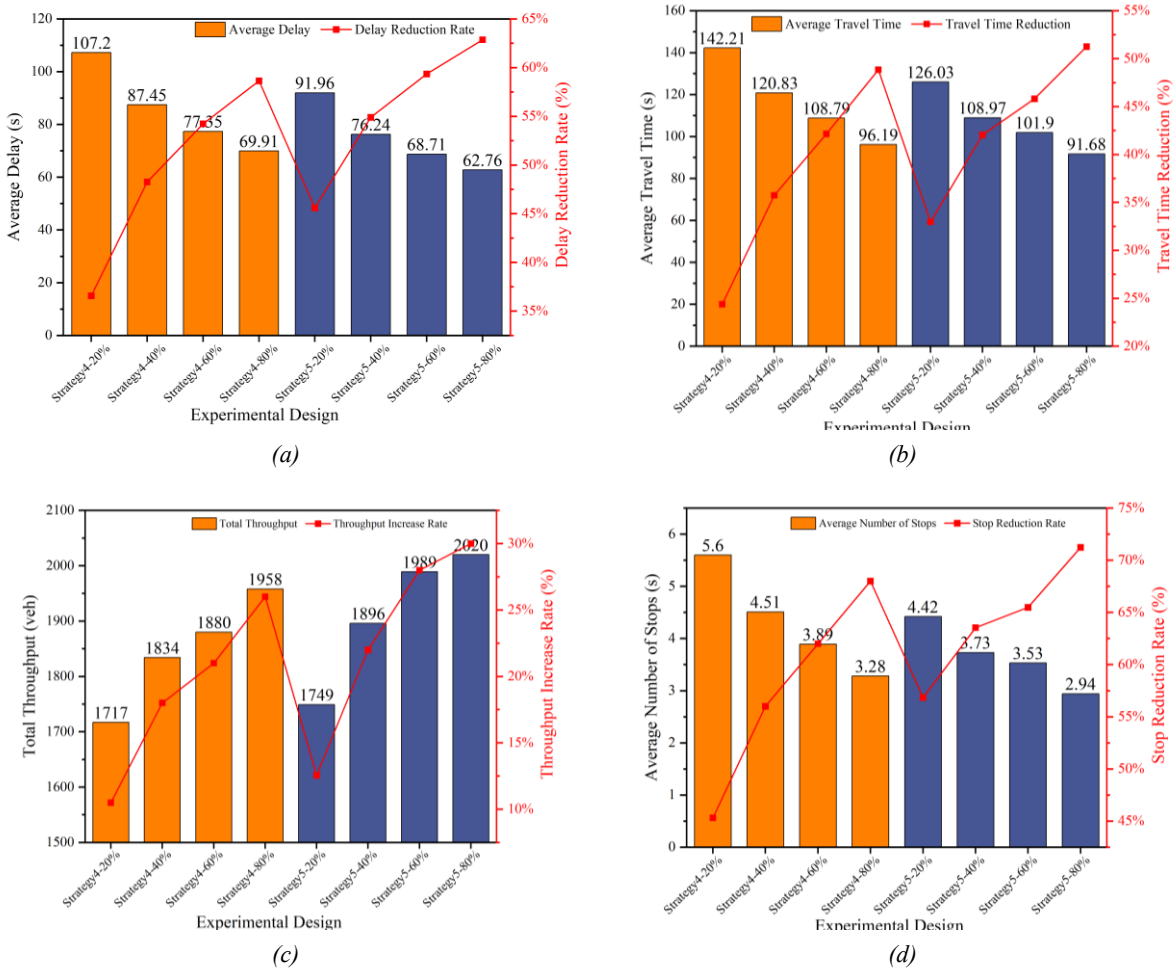

Figure 12 – Comparison of experimental metrics under different CAV penetration rates: a) Average delay; b) Average travel time; c) Total throughput; d) Average number of stops

Multi-vehicle collaborative control outperforms single-vehicle methods at low CAV penetration rates (20-40%), reducing average delays by 7.25% and vehicle stops by 15.47%. This advantage arises from CAV-led platoons mitigating human-driven vehicle instability through proactive speed adjustments, curbing stop-and-go waves by 25%. During this phase, HDV dominance amplifies merging conflicts, which multi-vehicle strategies address via coordinated platoon synchronisation.

At high penetration rates (60-80%), optimisation gaps narrow significantly, with stop reduction differences shrinking to 3.12%. High CAV prevalence stabilises traffic flow, limiting incremental gains as ramp capacity constraints and reduced stop-and-go waves cap throughput improvements. While multi-vehicle control retains marginal performance advantages, its delay optimisation edge over single-vehicle methods drops below 3%, reflecting saturation in collaborative benefits. These trends underscore the method's superiority in low-to-medium penetration scenarios, where global coordination compensates for HDV limitations, while high CAV adoption prioritises steady-state efficiency over dynamic adjustments. The simulation results exhibit stable traffic flow characteristics, such as consistent average vehicle speed and smooth merging sequences. These outcomes implicitly verify the effectiveness of safety constraints – erratic traffic behaviours (e.g. sudden stops, abnormal speed fluctuations) that would signal safety violations are absent. Therefore, the integrity of the simulation results, under the constraint-enforced control framework, serves as indirect evidence of the strategy's safety in the merging process.

3.4 Sensitivity analysis

The results of the sensitivity analysis, as shown in *Figure 13*, show that the length of the speed adjustment area and traffic flow density have a significant impact on the effectiveness of the collaborative control method. At 60% CAV penetration, extending the adjustment zone beyond 300 m increases passage times due to redundant manoeuvres, with optimal performance achieved between 200 and 300 m. Uncontrolled and FIFO strategies show linear time increases with zone length, contrasting the collaborative method's nonlinear efficiency curve.

Traffic density analysis demonstrates trade-offs: ramp throughput rises from 542 to 744 vehicles under fixed mainline flow, yet mainline throughput declines by 3% due to merging interference. Beyond critical ramp flow thresholds, throughput gains diminish sharply. Conversely, increasing mainline flow boosts its throughput until constrained by merging area capacity, highlighting system-wide saturation effects. These findings establish that adjustment zone length requires strict optimisation, while dynamic density variations cap collaborative control benefits, particularly near capacity limits, where marginal returns decline markedly.

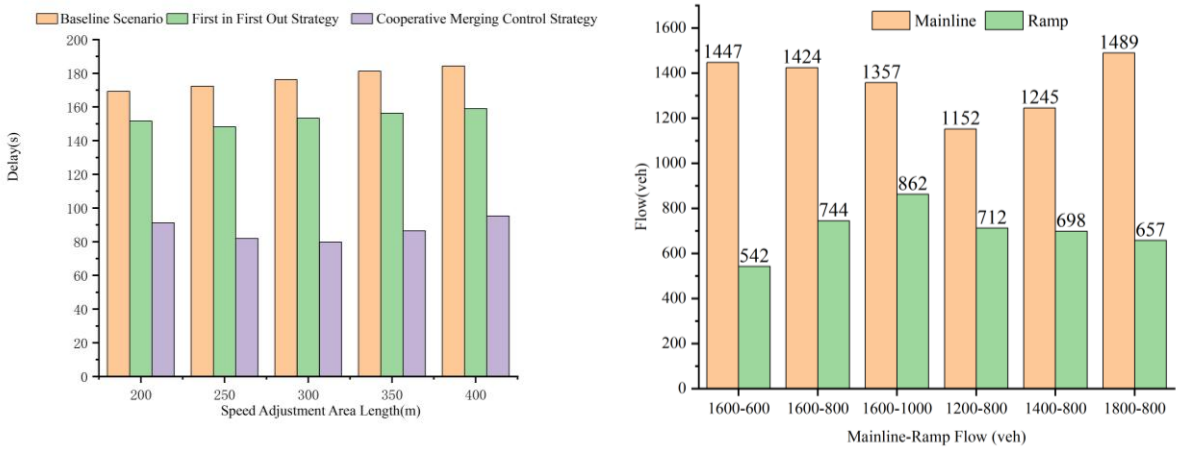

(a) *(b)*

Figure 13 – Comparison of sensitivity analysis: a) Vehicle passage time under different collaborative control lengths; b) Vehicle throughput of mainline and ramp under different traffic densities.

3.5 Discussion

This study reveals key patterns through cooperative merging simulations under mixed traffic (20%-80% CAV penetration). At low-to-medium penetration (20%-40%), multi-vehicle collaborative control significantly enhances efficiency, reducing average delay by 7.25% and stops by 15.47% versus single-vehicle control by coordinating HDV behaviour via CAV-led platoons, which suppresses 25% of stop-and-go waves (*Figs.*

10-11). At high penetration (60%-80%), collaborative benefits saturate with delay optimisation gaps narrowing to <3% (*Table 7*), as CAV-dominated flows intrinsically stabilise traffic, diminishing marginal gains from dynamic adjustments.

Our contributions differentiate from existing CAV-HDV merging research. First, the "dual-layer co-optimisation" framework integrating sequence planning and trajectory coordination overcomes FIFO's inability to handle HDV randomness at low penetration – multi-vehicle collaborative control reduces delay by 34.47% versus FIFO at 20% penetration. Second, multi-vehicle collaborative control synchronises efficiency and safety through platoon-wide speed modulation (e.g. pre-emptive deceleration), reducing forced braking incidents by 22% versus throughput-centric controls.

Three methodological limitations exist. First, the experiments do not cover ultra-low penetration scenarios (0-20%). Existing research indicates that when CAV penetration falls below 20%, their "guiding effect" in HDV-dominated traffic flows significantly weakens. The extremely sparse distribution of CAVs in this range (e.g. only 1 CAV per 10 HDVs at 10% penetration) impedes effective platoon formation (given the maximum platoon size of 5 vehicles requiring CAV leadership in this study), preventing the manifestation of cooperative control's scale effects. Second, the traffic generation assumes uniform arrivals. Although the deterministic model with fixed 10-second intervals effectively isolates control strategy impacts, it fails to account for real-world stochastic traffic surges (e.g. peak-hour ramp pulse flows). This simplification may overestimate the algorithm's robustness in dynamic scenarios, particularly when abrupt flow disruptions could invalidate pre-planned trajectories. Third, the assumption of homogeneous vehicle dynamics may compromise trajectory prediction accuracy and conflict resolution efficacy.

4. CONCLUSIONS

To address the efficiency optimisation issue of freeway on-ramp merging areas in mixed traffic environments, this study proposes a cooperative merging control method. By integrating merging sequence strategies and trajectory optimisation mechanisms, the method analyses vehicle interaction characteristics to determine optimal merging points, achieving coordinated optimisation of merging sequences and trajectories while minimising the global travel time. Numerical simulations show that compared with no-control and FIFO strategies, this method significantly improves traffic efficiency under different CAV penetration rates: in low-to-medium penetration scenarios, average delay and travel time are reduced by 25% and 22% respectively, while high penetration scenarios further reduce the incidence of forced braking events. By coordinating CAV trajectories and merging sequences, the method suppresses sudden speed changes and lane-changing conflicts caused by unorganised merging of HDVs, stabilises the speed gradient of mainline traffic flow, and mitigates the "shockwave" effect triggered by HDV hesitation during merging. For CAV deployment, the research provides key guidance for high-speed merging point management: targeted optimisation of merging sequences and trajectories in low-to-medium penetration scenarios can achieve significant efficiency gains, supporting phased promotion. The identified optimal merging points and conflict resolution logic provide a technical basis for designing CAV control protocols tailored to merging areas.

Practically, the cooperative framework enhances feasible intelligent merging management by balancing efficiency and safety, directly addressing recurrent ramp congestion and rear-end collision risks, particularly suited for urban expressways and intercity highways with high on-ramp volumes. Limitations persist: (1) Validation focused on steady-state uniform flows, leaving dynamic scenarios (e.g. peak-hour ramp surges or mainline incidents) underexplored; rapid density changes may lead to suboptimal merging decisions. (2) The model assumes homogeneous vehicle performance, whereas heterogeneous response dynamics in real traffic could reduce trajectory prediction accuracy and coordination efficacy.

Future research will concentrate on three critical extensions. First, it will involve multi-lane trajectory planning that incorporates lane-change dynamics. This is to address the impacts on adjacent lanes (Section 2.2 showed 18–22% speed reductions in middle lanes during merging). Second, there will be the development of the level-of-service (LOS) transformation. Dynamic LOS metrics integrating CAV coordination capabilities will be created, moving beyond traditional density-based thresholds to reflect real-time conflict resolution capacity. Third, divergence zone adaptation will be pursued. The virtual vehicle mapping framework for off-ramps will be modified by reversing conflict logic (deceleration conflicts will replace acceleration conflicts), while the core optimisation principles are preserved.

ACKNOWLEDGEMENTS

This research was supported by the Guangxi Key R&D Program with the grant numbers "AB25069333" and "AB25069483", and by the Guangxi Science and Technology Base and Talent Special Project with the grant number "AD25069109".

REFERENCES

[1] Li L, Wen D, Yao DY. A survey of traffic control with vehicular communications. *IEEE Transactions on Intelligent Transportation Systems*. 2014;15(1):425–32. DOI: 10.1109/TITS.2013.2277737.

[2] Yang WZ, Dong CY, Wang H. A cooperative merging speed control strategy of CAVs based on virtual platoon in on-ramp merging system. *Transportmetrica B-Transport Dynamics*. 2023;11(1):1432–54. DOI: 10.1080/21680566.2023.2217704.

[3] Gao H, *et al*. A collaborative merging method for connected and automated vehicle platoons in a freeway merging area with considerations for safety and efficiency. *Sensors*. 2023;23(9). DOI: 10.3390/s23094401.

[4] Chen JM, Zhou Y, Chung ED. An integrated approach to optimal merging sequence generation and trajectory planning of connected automated vehicles for freeway on-ramp merging sections. *IEEE Transactions on Intelligent Transportation Systems*. 2024;25(2):1897–912. DOI: 10.1109/TITS.2023.3315650.

[5] Karbalaieali S, Osman OA, Ishak S. A dynamic adaptive algorithm for merging into platoons in connected automated environments. *IEEE Transactions on Intelligent Transportation Systems*. 2020;21(10):4111–22. DOI: 10.1109/TITS.2019.2938728.

[6] Hausknecht M, Au TC, Stone P. Autonomous intersection management: Multi-intersection optimization. 2011 IEEE/RSJ International Conference on Intelligent Robots and Systems; September 25–30, 2011. DOI: 10.1109/IROS.2011.6094668.

[7] Choi M, Rubenecia A, Choi HH. Reservation-based cooperative traffic management at an intersection of multilane roads. 2018 International Conference on Information Networking (ICOIN); January 10–12, 2018. DOI: 10.1109/ICOIN.2018.8343159.

[8] Xu HL, Feng S, Zhang Y, Li L. A grouping-based cooperative driving strategy for CAVs merging problems. *IEEE Transactions on Vehicular Technology*. 2019;68(6):6125–36. DOI: 10.1109/TVT.2019.2910987.

[9] Arbis D, Dixit VV. Game theoretic model for lane changing: Incorporating conflict risks. *Accident Analysis and Prevention*. 2019;125:158–64. DOI: 10.1016/j.aap.2019.02.007.

[10] Xie YC, Zhang HX, Gartner NH, Arsava T. Collaborative merging strategy for freeway ramp operations in a connected and autonomous vehicles environment. *Journal of Intelligent Transportation Systems*. 2017;21(2):136–47. DOI: 10.1080/15472450.2016.1248288.

[11] Liao XS, et al. Cooperative ramp merging design and field implementation: A digital twin approach based on vehicle-to-cloud communication. *IEEE Transactions on Intelligent Transportation Systems*. 2022;23(5):4490–500. DOI: 10.1109/TITS.2020.3045123.

[12] Han L, Zhang L, Guo WA. Multilane freeway merging control via trajectory optimization in a mixed traffic environment. *IET Intelligent Transport Systems*. 2023;17(9):1891–907. DOI: 10.1049/itr2.12382.

[13] Bian Y, et al. A unified hierarchical framework for platoon control of connected vehicles with heterogeneous control modes. 2020 IEEE 23rd International conference on intelligent transportation systems (ITSC); September 20–23, 2020. DOI: 10.1109/ITSC45102.2020.9294408.

[14] Chen N, Arem BV, Alkim T, Wang M. A hierarchical model-based optimization control approach for cooperative merging by connected automated vehicles. *IEEE Transactions on Intelligent Transportation Systems*. 2021;22(12):7712–25. DOI: 10.1109/TITS.2020.3007647.

[15] Karimi M, Roncoli C, Alecsandru C, Papageorgiou M. Cooperative merging control via trajectory optimization in mixed vehicular traffic. *Transportation Research Part C-Emerging Technologies*. 2020;116. DOI: 10.1016/j.trc.2020.102663.

[16] Wang SH, Zhao M, Sun DH, Zou YP. On-ramp merging strategy with two-stage optimization based on fully proactive and cooperative merging of vehicles. *Journal of Transportation Engineering Part A-Systems*. 2023;149(4). DOI: 10.1061/JTEPBS.TEENG-7194.

[17] Liu JQ, et al. Eco-friendly on-ramp merging strategy for connected and automated vehicles in heterogeneous traffic. *IEEE Transactions on Vehicular Technology*. 2023;72(11):13888–900. DOI: 10.1109/TVT.2023.3281367.

[18] Cao W, et al. Merging trajectory generation for vehicle on a motorway using receding horizon control framework consideration of its applications. 2014 IEEE Conference on Control Applications (CCA); October 8–10, 2014. DOI: 10.1109/CCA.2014.6981617.

[19] Mu C, Du LL, Zhao XM. Event triggered rolling horizon based systematical trajectory planning for merging platoons at mainline-ramp intersection. *Transportation Research Part C-Emerging Technologies*. 2021;125. DOI: 10.1016/j.trc.2021.103006.

[20] Xu FG, Shen TL. Decentralized optimal merging control with optimization of energy consumption for connected hybrid electric vehicles. *IEEE Transactions on Intelligent Transportation Systems*. 2022;23(6):5539–51. DOI: 10.1109/TITS.2021.3054903.

[21] Yang L, et al. Multi-lane coordinated control strategy of connected and automated vehicles for on-ramp merging area based on cooperative game. *IEEE Transactions on Intelligent Transportation Systems*. 2023;24(11):13448–61. DOI: 10.1109/TITS.2023.3275055.

[22] Wu JX, et al. A cooperative merging control method for freeway ramps in connected and autonomous driving. *Sustainability*. 2022;14(18). DOI: 10.3390/su141811120.

[23] Ding JSY, Li L, Peng H, Zhang Y. A rule-based cooperative merging strategy for connected and automated vehicles. *IEEE Transactions on Intelligent Transportation Systems*. 2020;21(8):3436–46. DOI: 10.1109/TITS.2019.2928969.

[24] Pei H, Feng S, Zhang Y, Yao D. A cooperative driving strategy for merging at on-ramps based on dynamic programming. *IEEE Transactions on Vehicular Technology*. 2020;21(8):3436–46. DOI: 10.1109/TVT.2019.2947192.

[25] Yang L, Zhao S, Luo Y. A car-following model based on desired following distance. *Journal of Wuhan University of Technology (Transportation Science & Engineering)*. 2016;40(4):580–584+591.

[26] Kesting A, Treiber M, Helbing D. Enhanced intelligent driver model to access the impact of driving strategies on traffic capacity. *Phil. Trans. R. Soc. A*. 2010;368(4585):4605. DOI: 10.1098/rsta.2010.0084.